

RECEIVED

JUN 05 1998

OSTI

NUREG/CR-6509
BNL-NUREG-52515

The Effect of Initial Temperature on Flame Acceleration and Deflagration-to-Detonation Transition Phenomenon

Prepared by
G. Ciccarelli, J.L. Boccio, T. Ginsberg, C. Finfrock, L. Gerlach/BNL
H. Tagawa/NUPEC
A. Malliakos/NRC

Brookhaven National Laboratory

**Prepared for
U.S. Nuclear Regulatory Commission**

and

Nuclear Power Engineering Corporation



AVAILABILITY NOTICE

Availability of Reference Materials Cited in NRC Publications

Most documents cited in NRC publications will be available from one of the following sources:

1. The NRC Public Document Room, 2120 L Street, NW., Lower Level, Washington, DC 20555-0001
2. The Superintendent of Documents, U.S. Government Printing Office, P. O. Box 37082, Washington, DC 20402-9328
3. The National Technical Information Service, Springfield, VA 22161-0002

Although the listing that follows represents the majority of documents cited in NRC publications, it is not intended to be exhaustive.

Referenced documents available for inspection and copying for a fee from the NRC Public Document Room include NRC correspondence and internal NRC memoranda; NRC bulletins, circulars, information notices, inspection and investigation notices; licensee event reports; vendor reports and correspondence; Commission papers; and applicant and licensee documents and correspondence.

The following documents in the NUREG series are available for purchase from the Government Printing Office: formal NRC staff and contractor reports, NRC-sponsored conference proceedings, international agreement reports, grantee reports, and NRC booklets and brochures. Also available are regulatory guides, NRC regulations in the *Code of Federal Regulations*, and *Nuclear Regulatory Commission Issuances*.

Documents available from the National Technical Information Service include NUREG-series reports and technical reports prepared by other Federal agencies and reports prepared by the Atomic Energy Commission, forerunner agency to the Nuclear Regulatory Commission.

Documents available from public and special technical libraries include all open literature items, such as books, journal articles, and transactions. *Federal Register* notices, Federal and State legislation, and congressional reports can usually be obtained from these libraries.

Documents such as theses, dissertations, foreign reports and translations, and non-NRC conference proceedings are available for purchase from the organization sponsoring the publication cited.

Single copies of NRC draft reports are available free, to the extent of supply, upon written request to the Office of Administration, Distribution and Mail Services Section, U.S. Nuclear Regulatory Commission, Washington, DC 20555-0001.

Copies of industry codes and standards used in a substantive manner in the NRC regulatory process are maintained at the NRC Library, Two White Flint North, 11545 Rockville Pike, Rockville, MD 20852-2738, for use by the public. Codes and standards are usually copyrighted and may be purchased from the originating organization or, if they are American National Standards, from the American National Standards Institute, 1430 Broadway, New York, NY 10018-3308.

DISCLAIMER NOTICE

This report was prepared as an account of work sponsored by an agency of the United States Government. Neither the United States Government nor any agency thereof, nor any of their employees, makes any warranty, expressed or implied, or assumes any legal liability or responsibility for any third party's use, or the results of such use, of any information, apparatus, product, or process disclosed in this report, or represents that its use by such third party would not infringe privately owned rights.

DISCLAIMER

This report was prepared as an account of work sponsored by an agency of the United States Government. Neither the United States Government nor any agency thereof, nor any of their employees, makes any warranty, express or implied, or assumes any legal liability or responsibility for the accuracy, completeness, or usefulness of any information, apparatus, product, or process disclosed, or represents that its use would not infringe privately owned rights. Reference herein to any specific commercial product, process, or service by trade name, trademark, manufacturer, or otherwise does not necessarily constitute or imply its endorsement, recommendation, or favoring by the United States Government or any agency thereof. The views and opinions of authors expressed herein do not necessarily state or reflect those of the United States Government or any agency thereof.

The Effect of Initial Temperature on Flame Acceleration and Deflagration-to-Detonation Transition Phenomenon

Manuscript Completed: April 1998

Date Published: May 1998

Prepared by

G. Ciccarelli, J.L. Boccio, T. Ginsberg, C. Finfrock, L. Gerlach, Brookhaven National Laboratory

H. Tagawa, Nuclear Power Engineering Corporation

A. Malliakos, U.S. Nuclear Regulatory Commission

Brookhaven National Laboratory

Upton, NY 11973-5000

A. Malliakos, NRC Project Manager

Prepared for

Division of Systems Technology

Office of Nuclear Regulatory Research

U.S. Nuclear Regulatory Commission

Washington, DC 20555-0001

NRC Job Code L1924/A3991

DISTRIBUTION OF THIS DOCUMENT IS UNLIMITED

pjh

and

Nuclear Power Engineering Corporation
5F Fujita Kanko Toranomon Building
3-17-1, Toranomon, Minato-Ku
Tokyo 105
Japan

MASTER



ABSTRACT

The High-Temperature Combustion Facility at BNL was used to conduct deflagration-to-detonation transition (DDT) experiments. Periodic orifice plates were installed inside the entire length of the detonation tube in order to promote flame acceleration. The orifice plates are 27.3-cm-outer diameter, which is equivalent to the inner diameter of the tube, and 20.6-cm-inner diameter. The detonation tube length is 21.3-meters long, and the spacing of the orifice plates is one tube diameter. A standard automobile diesel engine glow plug was used to ignite the test mixture at one end of the tube. Hydrogen-air-steam mixtures were tested at a range of temperatures up to 650K and at an initial pressure of 0.1 MPa.

In most cases, the limiting hydrogen mole fraction which resulted in DDT corresponded to the mixture whose detonation cell size, λ , was equal to the inner diameter of the orifice plate, d (e.g., $d/\lambda=1$). The only exception was in the dry hydrogen-air mixtures at 650K where the DDT limit was observed to be 11 percent hydrogen, corresponding to a value of d/λ equal to 5.5. For a 10.5 percent hydrogen mixture at 650K, the flame accelerated to a maximum velocity of about 120 m/s and then decelerated to below 2 m/s. By maintaining the first 6.1 meters of the vessel at the ignition end at 400K, and the rest of the vessel at 650K, the DDT limit was reduced to 9.5 percent hydrogen ($d/\lambda=4.2$). This observation indicates that the $d/\lambda=1$ DDT limit criteria provides a necessary condition but not a sufficient one for the onset of DDT in obstacle laden ducts. In this particular case, the mixture initial condition (i.e., temperature) resulted in the inability of the mixture to sustain flame acceleration to the point where DDT could occur.

It was also observed that the distance required for the flame to accelerate to the point of detonation initiation, referred to as the run-up distance, was found to be a function of both the hydrogen mole fraction and the mixture initial temperature. Decreasing the hydrogen mole fraction or increasing the initial mixture temperature resulted in longer run-up distances. The density ratio across the flame and the speed of sound in the unburned mixture were found to be two parameters which influence the run-up distance.

CONTENTS

ABSTRACT	iii
LIST OF FIGURES	vi
LIST OF TABLES	viii
EXECUTIVE SUMMARY	ix
ACKNOWLEDGMENTS	xi
1 INTRODUCTION	1
2 DDT PHENOMENA - A BRIEF OVERVIEW	3
3 EXPERIMENTAL DETAILS	9
4 EXPERIMENTAL RESULTS	12
4.1 Flame Propagation Regimes	12
4.1.1 Detonation Regime	12
4.1.2 Choking Regime	13
4.1.3 Slow Deflagration	13
4.2 Flame Propagation Regimes at 300K	14
4.3 Flame Propagation Regimes at 500K	15
4.4 Flame Propagation Regimes at 650K	17
4.5 Flame Propagation Regimes in Hydrogen-Air-Steam Mixtures	19
4.6 Detonation Run-Up Distance	20
5 DISCUSSION	40
5.1 Flame Acceleration	40
5.1.1 Flame Acceleration Mechanism	40
5.1.2 Influence of Initial Temperature on Flame Acceleration Parameters	43
5.2 DDT Limit Criterion	46
5.3 Influence of Detonation Stability	48
6 CONCLUSION	52
7 REFERENCES	54
APPENDIX A	A-1

FIGURES

Figure No.		Page No.
2.1	Schematic showing the steady-state flame propagation regimes	8
3.1	Photograph of the HTCF Detonation Vessel	10
3.2	Schematic of Orifice Plate Geometry and Dimensions	11
4.1	Combustion Front Velocity Versus Propagation Distance in Three Hydrogen-Air Mixtures at 300K and 0.1 MPa	22
4.2	Typical Pressure Time History Corresponding to a; (a) Detonation Wave (b) Deflagration in the Choking Regime	23
4.3	Combustion Front Velocity Versus Hydrogen Mole Fraction for Hydrogen-Air Mixtures at 300K and 0.1 MPa.	24
4.4	Comparison of the Measured Peak Overpressure for Hydrogen-Air Mixtures at 300K and 0.1 MPa and the Theoretical AICC and CJ Detonation Pressure	25
4.5	Combustion Front Velocity Versus Propagation Distance in Three Hydrogen-Air Mixtures at 500K and 0.1 MPa	26
4.6	Combustion Front Velocity Versus Hydrogen Mole Fraction for Hydrogen-Air Mixtures at 500K and 0.1 MPa.	27
4.7	Comparison of the Measured Peak Overpressure for Hydrogen-Air Mixtures at 500K and 0.1 MPa and the Theoretical AICC and CJ Detonation Pressure	28
4.8	Combustion Front Velocity Versus Propagation Distance in Four Hydrogen-Air Mixtures at 650K and 0.1 MPa	29
4.9	Combustion Front Velocity Versus Hydrogen Mole Fraction for Hydrogen-Air Mixtures at 650K and 0.1 MPa.	30
4.10	Comparison of the Measured Peak Overpressure for Hydrogen-Air Mixtures at 650K and 0.1 MPa and the Theoretical AICC and CJ Detonation Pressure	31
4.11	Combustion Front Velocity for a 11 Percent Hydrogen in Air Mixture at Four Different Initial	32
4.12	Combustion Front Velocity Versus Hydrogen Mole Fraction for Hydrogen-Air Mixtures at 650K and 0.1 MPa with the First Six Meters of the Vessel Maintained at 400K.	33
4.13	Combustion Front Velocity Versus Hydrogen Mole Fraction for Hydrogen-Air Mixtures with 10 Percent Steam at 400K and 0.1 MPa	34
4.14	Combustion Front Velocity Versus Hydrogen Mole Fraction for Hydrogen-Air Mixtures with 25 Percent Steam at 500K and 0.1 MPa	35
4.15	Combustion Front Velocity Versus Hydrogen Mole Fraction for Hydrogen-Air Mixtures with 25 Percent Steam at 650K and 0.1 MPa	36
4.16	Combustion Front Velocity Versus Propagation Distance in Three Hydrogen-Air Mixtures with 25 Percent Steam at 650K and 0.1 MPa	37

FIGURES

(Continued)

Figure No.		Page No.
4.17	Combustion Front Velocity Versus Hydrogen Mole Fraction for Hydrogen-Air Mixtures with 25 Percent Steam at 650K and 0.1 MPa with the First Six Meters of the Vessel Maintained at 400K	38
4.18	Measured Detonation Run-Up Distance for Hydrogen-Air Mixtures at Three Initial Temperatures	39
5.1	Schematic Showing Flame Propagation in a Closed-Ended Tube with Appropriate Nomenclature Indicated	49
5.2	Schematic Showing the Velocity Flow Field Generated Ahead of a Flame Propagating in an Obstacle-Laden Tube	50
5.3	Schematic Showing Flame and Unburnt Flow Velocity Vectors in the (a) Fixed Reference Frame and (b) Reference Frame Moving with the Flame	51

TABLES

Table No.		Page No.
2.1	Experimental DDT Limit Data from Guirao et al., 1989	5
5.1	Density Ratio Across the Flame and the Laminar Burning Velocity as a Function of Temperature and Mixture Composition	44
5.2	Speed of Sound in the Unburnt Mixture	45
A.1	Summary of initial thermodynamic conditions and measured combustion front velocity and pressure	A-2

EXECUTIVE SUMMARY

This report provides experimental results obtained at Brookhaven National Laboratory (BNL) from the High-Temperature Hydrogen Combustion Research Program which is jointly funded by the U.S. Nuclear Regulatory Commission and the Japanese Nuclear Power Engineering Corporation (NUPEC), sponsored by the Ministry of International Trade and Industry (MITI). The objective of this program is to study high-speed combustion phenomenon in hydrogen-air-steam mixtures at high initial temperature which could occur in a nuclear power plant during a severe accident scenario. The High-Temperature Combustion Facility was constructed at BNL with the unique capability of studying high-temperature detonation phenomena. This is a multiphase program designed to investigate the effects of initial temperature on detonation phenomena in hydrogen-air-steam mixtures. The program includes the investigation of DDT phenomenon at high temperature with and without venting. This report provides the results obtained in the study of DDT phenomenon without venting, and a separate report will be published which deals with the venting experiments.

The maximum pressure achievable by a relatively slow deflagration, in an enclosed environment, is the Adiabatic Isochoric Complete Combustion (AICC) pressure. Under the appropriate conditions a deflagration could lead to the initiation of a detonation wave. A detonation wave is more of a threat to the integrity of a nuclear power plant containment (Berman, 1982) than a deflagration. This is because for a detonation wave the dynamic shock pressure is typically twice the AICC pressure, and the reflected detonation pressure is roughly five times the AICC pressure. A key question when predicting pressure loads in a nuclear reactor containment building resulting from a hydrogen burn is the likelihood that a detonation can be generated from an accelerating flame. The DDT experimental results reported here provide some insight into the effect of initial temperature on the flame acceleration process that leads to the onset of a detonation and the conditions required for detonation to develop.

The HTCF consists of a detonation tube which can be heated to a maximum temperature of 700K with a temperature uniformity of $\pm 14K$. The detonation tube is 21.3-meters long and is constructed from stainless steel pipe with an internal diameter of 27.3 cm. Instrumentation ports are located at regular intervals of 0.61 meters. The test mixture is blended inside of a mixing chamber fed by two pipes, one flowing room temperature air and the other a heated mixture of hydrogen and steam. The desired mixture composition is achieved by varying the individual constituent flow rates via choked venturis.

To experimentally investigate DDT, a flame is initiated at one end of the tube, subsequently accelerating as a result of turbulence generated in the induced flow ahead of the flame. For certain mixtures, this flame acceleration could lead to the initiation of a detonation wave. In order to promote flame acceleration, periodic orifice plates were installed down the length of the entire detonation tube. The orifice plates have an outer diameter of 27.3 cm, which is equivalent to the inner diameter of the tube, an inner diameter of 20.6 cm, and a spacing of one tube diameter. A standard automobile diesel engine glow plug was used to ignite the test mixture at one end of the tube.

Flame propagation in this geometry usually consists of an initial flame acceleration phase followed by a steady-state phase. The various flame propagation regimes have been classified as: (1) detonation, (2) choking, and (3) slow deflagrations. In the detonation regime, flame acceleration leads to the initiation of a detonation which propagates at a velocity typically just under the theoretical detonation velocity. In the choking regime, the final steady-state velocity equals the speed of sound in the burnt gas. For lean mixtures

above the flammability limit and below the choking limit, the flame accelerates to a maximum velocity on the order of 100-200 m/s and then decelerates to a velocity roughly equal to the laminar burning velocity, which we refer to as slow deflagrations.

In terms of potential pressure loads resulting from a hydrogen burn, the slow deflagration mode is the least severe since the pressure rises very slowly and there is no dynamic shock loading. The detonation mode is the most severe; however, flame propagation in the choking regime can also be significant due to the shock loading. In fact, the peak shock pressures which are typically close to the AICC pressure are comparable to the pressure measurements made in lean mixtures in the detonation regime.

In general, for the tube diameter and orifice plate configuration studied, it was found that increasing the initial temperature of hydrogen-air-steam mixtures at 0.1 MPa increased the likelihood of DDT. For example, DDT was not observed in mixtures of hydrogen-air between 11 and 14 percent hydrogen at an initial temperature of 300K, whereas, DDT was observed for these same mixtures at 650K.

In most cases, flame propagation in the detonation regime was observed in hydrogen-air-steam mixtures with a detonation cell size, λ , smaller than the inner diameter of the orifice plates, d . Therefore, the transition from the choking regime to the detonation regime occurs at the mixture whose detonation cell size equals the inner diameter of the orifice plates (e.g., $d/\lambda=1$). These experimental observations are consistent with previous work done looking at DDT phenomenon in obstacle-laden tubes at room temperature. In the present study, the only exception was in the dry hydrogen-air mixtures at 650K. At 650K, a d/λ of at least 5.5 (i.e., corresponding to an 11 percent hydrogen in air mixture) was required for detonation transition. For a 10.5 percent hydrogen mixture, flame propagation was in the slow deflagration regime, and there was no propagation in the choking regime. This indicates that the $d/\lambda=1$ DDT limit criteria provides a necessary but not sufficient condition for the onset of DDT in obstacle laden duct.

It was also observed that the distance required for the flame to accelerate to the point of detonation initiation, referred to as the run-up distance, was found to be a function of both the hydrogen mole fraction and the mixture initial temperature. Decreasing the hydrogen mole fraction or increasing the initial mixture temperature resulted in longer run-up distances. The density ratio across the flame and the speed of sound in the unburned mixture were found to be the two parameters which influence the run-up distance.

ACKNOWLEDGMENTS

The authors would like to acknowledge the technical guidance provided by Dr. John Lee of McGill University and Dr. Joseph Shepherd of the California Institute of Technology. We have frequently drawn upon their experience in the field of detonation physics and gained from many fruitful discussions.

We would also like to acknowledge the review of the report performed by Dr. Hideo Ogasawara and Mr. Takashi Hashimoto of the Nuclear Power Engineering Corporation, Tokyo, Japan.

This study was performed within the Safety and Risk Evaluation Division of the Department of Advanced Technology, Brookhaven National Laboratory. The administrative support of Dr. W. T. Pratt, Division Head, and Dr. R. A. Bari, Department Head, are much appreciated.

The authors would also like to thank Ms. Jean Frejka for her continued assistance in the administrative aspects of the project, and with her, Ms. Alice Jimenez-Costantini, for their help in the preparation of this report.

1. INTRODUCTION

One of the safety concerns for light-water nuclear reactors is the possibility of the development and ignition of a combustible hydrogen-air-steam atmosphere inside the containment building during a severe accident. One of the consequences of an accident involving core degradation is the production of combustible quantities of hydrogen from metal-water reactions. In the Three-Mile Island accident, where hydrogen was released from the degraded core, it has been postulated that the 0.19 MPa overpressure spike measured inside the containment building was the result of a relatively slow hydrogen burn (Berman, 1982). This pressure spike was well below the 0.4 MPa design overpressure of the containment, and, therefore, its structural integrity was not challenged.

It is generally acknowledged, however, that the integrity of a containment building could be threatened during a severe accident by a supersonic mode of combustion, referred to as a detonation wave (Berman, 1982). In the classical description, a detonation wave is a mode of combustion where the flame (i.e., reaction zone) is preceded by a planar shock wave. The shock wave adiabatically compresses the combustible gas raising the temperature to the point where chemical reactions proceed very quickly. A detonation wave is self-sustained since the energy released by the chemical reactions supports the shock wave. The detonation shock pressure is typically twice the Adiabatic Isochoric, Complete Combustion (AICC) pressure, which is the maximum pressure achievable in an enclosure by a slow deflagration, and the reflected wave pressure is roughly five times the AICC pressure. A detonation wave could be initiated directly by a point source of energy. However, considering the large amount of energy required for direct initiation of a detonation in prototypic mixtures, the point source initiation of a detonation in most severe accident scenarios is unrealistic.

A more likely scenario for detonation initiation would be the ignition of a slow deflagration followed by flame acceleration leading to detonation. Such a phenomenon is referred to as Deflagration-to-Detonation Transition (DDT), and it can have a very pronounced effect on the pressure loading on the containment walls. In a closed volume such as the reactor containment, the pressure loading time history on the containment walls depends on the run-up distance (also called induction distance or pre-detonation distance) for the deflagration leading to the onset of detonation. For example, for a very long run-up distance, the ambient pressure in the enclosure increases as a result of the accelerating flame before the detonation is initiated. This increase in pressure is due to the reduction in the containment average gas density as more fresh gas is converted to hot combustion products. This results in a detonation with a higher peak pressure due to the higher initial mixture pressure. For a short run-up distance, the ambient pressure does not change much, but the impulse associated with the subsequent detonation wave increases due to the longer detonation propagation distance (Nettleton, 1987). Locally, at the point of DDT, the detonation is overdriven and the peak pressure is typically much higher than the normal detonation pressure. If DDT occurs close to the containment wall, this would result in very high local pressure loading.

Most postulated severe accident scenarios are characterized by containment atmospheres of about 373K and up to 0.3 MPa. However, calculations have shown that under certain accident scenarios local compartment temperatures in excess of 373K are predicted (Yang, 1992). Since little DDT experimental data exists at such temperatures, the need arose to perform further investigations into the DDT process at prototypic severe accident conditions.

The High-Temperature Hydrogen Combustion Research Program at Brookhaven National Laboratory is a jointly funded program by the U.S. Nuclear Regulatory Commission and the Japanese Nuclear Power

1. Introduction

Engineering Corporation (NUPEC), sponsored by the Ministry of International Trade and Industry (MITI). The overall objective of the program is to extend the ability to assess potential detonation type loads in containment during a postulated severe accident characterized by initial high-temperature hydrogen-air mixtures with large steam dilution. Results obtained in the first element of the program, focussing on measurement of detonation cell size, were reported in NUREG/CR-6213 and NUREG/CR-6391. This report presents results on the effect of initial temperature on DDT phenomenon in hydrogen-air and steam mixtures.

The objective of the present set of experiments is to characterize the effect of mixture initial temperature on flame acceleration and most importantly on the potential for DDT. Using the cell size data for hydrogen-air-steam at elevated temperatures reported in Ciccarelli et al. (1994, 1997), the purpose of this series of experiments is to determine if the criterion for detonation transition, obtained under "low" temperature conditions, applies at elevated initial temperatures up to 650K.

2. DDT PHENOMENA - A BRIEF OVERVIEW

In order to initiate a detonation directly, a large amount of energy is required to be deposited in a very short time so as to generate a strong blast wave. To initiate the detonation the blast wave must be capable of initiating chemical reactions in the mixture on a time scale comparable to the chemical reaction time scale associated with a detonation (i.e., tens of microseconds). At room temperature and pressure, one gram of high explosive (i.e., Tetral) is required to directly initiate a detonation in a stoichiometric mixture of hydrogen-air at standard temperature and pressure. This value goes up to 36 grams of Tetral for a hydrogen-air mixture containing 17.4 percent hydrogen (Guirao et al., 1989). It is generally accepted that in a nuclear reactor direct initiation of a detonation is highly improbable due to the nonexistence of such high energy sources.

The classical structure of a detonation wave consists of a planar shock wave followed by a reaction zone where energy released supports the shock wave. The coupled shock wave reaction zone propagates at the Chapman-Jouget (CJ) velocity which can be calculated theoretically knowing the mixture energetics. The corresponding detonation pressure is referred to as the CJ pressure. The actual structure of a detonation wave consists of a series of finite-amplitude transverse waves which interact with the leading shock wave. The collision of these transverse waves is essential to the propagation of the detonation wave. The average spacing between these transverse waves is referred to as the detonation "cell size" (Ciccarelli et al, 1994, 1997). The cell size, which is unique for each detonable mixture, has been correlated with the calculated 1-dimensional induction zone length, using the classical ZND detonation model (Shepherd, 1986). The detonation cell size can be considered to be the characteristic length scale for a detonation wave. Lee (1984) proposed, and has since been demonstrated for most mixtures of practical concern, that the cell size is a fundamental "dynamic parameter" which governs detonation phenomena, such as propagation limits and initiation energy.

If a combustible mixture is confined in a relatively long and narrow duct, it is possible that a flame ignited by a weak spark or hot surface can accelerate and initiate a detonation. As the flame propagates in a laterally confined space, the combustible gas ahead of the flame is pushed forward due to the increase in the specific volume across the flame. Initially, the flame is laminar and flame acceleration during this stage is due to increased flame surface area. As the flow velocity ahead of the flame increases, it becomes turbulent causing the flame surface to become wrinkled and the local burning velocity increase due to the enhanced turbulent transport properties. The enhanced burning velocity increases the flame velocity and thus the flow velocity ahead of the flame, which leads to increased turbulence intensity and thus to a larger burning velocity. In this way, a positive feedback mechanism is established which leads to flame acceleration. As the flame accelerates to speeds approaching the speed of sound in the fresh mixture, compression waves are produced ahead of the flame. Over time, these compression waves coalesce producing a shock wave ahead of the flame. If this shock wave attains sufficient strength, a detonation can form in the compressed gas between the flame and the shock. Of particular interest to the chemical and process industry, which typically handle combustible mixtures in long pipelines, is data on the distance between the ignition of the flame and the formation of the detonation wave. This flame acceleration distance is commonly referred to as the detonation run-up distance or the induction distance. Run-up distances in smooth tubes have been studied for a variety of combustible mixtures including hydrogen-air (Bollinger, 1964). The run-up distance was found to be a minimum for stoichiometric mixtures. The effect of initial mixture temperature on the run-up distance was first studied by Lafitte (1928) and later by Bollinger et al. (1961). In both these studies, it was shown that the run-

2. DDT Phenomena

up distance increases with increased initial temperature, possibly due to the effects of temperature on burning velocity, sound speed and turbulence structure.

A detailed investigation of the DDT process resulting from accelerating flames in smooth ducts was performed by the Berkley group in the late 1960s headed by Oppenheim. Using stroboscopic laser-schlieren, Oppenheim photographed the final stages of flame acceleration leading to DDT (Uriew and Oppenheim, 1966). The photographs clearly show a train of compression waves generated by the turbulent flame which coalesce into a strong leading shock wave. The photographs indicated that DDT, or the so-called "explosion within the explosion," always occurred within the shock-flame complex.

Flame acceleration in a duct can be enhanced by the roughening of the duct walls or the presence of obstacles in the flow field. Obstacles generate gradients in the flow field ahead of the flame resulting in large-scale "flame folding". The increased flame surface area increases the turbulent burning rate, and as discussed above, this leads to an increase in the flow velocity ahead of the flame and consequently flame acceleration. Superimposed on the large-scale flame fold are small-scale shear layers produced at the obstacle edges which also promote flame acceleration. It has been observed that a turbulent flame in an obstacle laden duct generates compression waves ahead of it much like in the smooth duct. The local high temperature and pressure generated by the reflection of the leading shock wave off an obstacle face is typically the location for detonation initiation. Detonation initiation due to shock reflection has been investigated in detail in the past (Meyer and Oppenheim, 1971). Teodorczyk et al. (1991) demonstrated using schlieren photography that while the obstacle face provides a source for detonation initiation via shock reflection, it is also a source of local detonation failure caused by wave diffraction around the obstacle.

The exact mechanism by which a detonation is formed has yet to be conclusively identified. The Shock Wave Amplification by Coherent Energy Release (SWACER) mechanism has been proposed by Lee et al. (1978) to describe the process by which spatial nonuniformities in the chemical induction time in a mixture can result in the formation of a detonation. In essence, the chemical energy release must be in phase with an expanding pressure wave so as to amplify it to a strength consistent with a detonation wave. In the case of DDT resulting from flame acceleration, the nonuniformities can be due to local fluctuations in the compressed region between the flame and the leading shock wave. The induction time gradient required for the SWACER mechanism to be effective can result from temperature gradients generated from local turbulent mixing of combustion products and fresh mixture.

A large body of experimental data exists in the literature dealing with flame acceleration and DDT phenomenon. As discussed above, initially most of the studies dealing with flame acceleration and DDT were performed in smooth tubes. The pioneering work on the influence of obstacles on flame acceleration was carried out by Chapman and Wheeler (1926) and on DDT by Shchelkin (1940). In the early 1980s, a joint program between McGill University and Sandia National Laboratory was undertaken to investigate flame acceleration in confined hydrogen-air mixtures. Small-scale tests were performed at McGill using long tubes with diameters of 5, 15, and 30 cm (Guirao et al., 1989). In these tests, an array of orifice plates were placed inside the tubes to promote turbulence and thus flame acceleration. The intent of this configuration was not to simulate any structure which exists in a nuclear power plant. The results from this simple geometry was used to characterize the flame acceleration and DDT processes. The roughness of the tube is controlled by the blockage ratio (BR) of the orifice plate defined as $BR = 1 - (d/D)^2$ where d and D are the inner and outer

2. DDT Phenomena

diameters of the orifice plate (note D is also equal to the inner diameter of the tube). It was determined that the greatest flame acceleration resulted for a blockage ratio of about 0.43 and an orifice spacing of one tube diameter.

In a typical experiment, flame acceleration takes place in the first few meters of the tube, usually followed by steady-state flame propagating to the end of the tube. The combustion front propagation in the final steady-state phase was classified as "choking" and "quasi-detonation" regimes (Guirao et al., 1989) based on the final steady-state flame velocity. These two regimes can be identified if one plots the final average flame velocity versus the hydrogen mole fraction, as shown schematically in Figure 2.1.

In the choking regime, the flame accelerates to a final steady-state velocity which is close to the isobaric sound speed in the products assuming a constant pressure combustion process. It is argued that the maximum steady-state flame velocity achievable is the speed of sound in the products due to choking of the flow as a result of heat addition from combustion. It has recently been proposed by Chu et al. (1993), based on theoretical considerations, that flame propagation in the choking regime could be described as a plane precursor shock wave driven by a CJ deflagration. In a CJ deflagration, the velocity of the products is sonic relative to the flame (i.e., CJ condition). Since in a closed-ended tube the products are at rest relative to the tube, this implies that the flame propagates at the speed of sound of the products. For a given mixture, there is a unique shock strength which results in flame velocity which satisfies the CJ condition. In all cases, the shock wave velocity is slightly faster than the flame velocity, and as such, the distance between the flame and the shock increases in time. This is in contrast to a 1-dimensional CJ detonation wave where the distance between the flame and the leading shock wave, or the reaction zone length, is small and remains constant.

In the quasi-detonation regime, flame acceleration leads to transition to detonation. The term quasi-detonation is used in place of simply detonation because after DDT the detonation propagates at a velocity well below the theoretical CJ velocity for the mixture. The detonation sub-CJ velocity is due to severe momentum and heat losses imposed on the detonation by the repeated orifice plates. The leanest hydrogen-air mixture which resulted in DDT (i.e., DDT limit) in each of the three different McGill tubes having a BR of 0.43 are given in the following table.

Table 2.1 Experimental DDT limit data

Tube I.D.; D (cm)	Orifice I.D.; d (cm)	Minimum H ₂ (%)	Cell size; λ (cm)	λ/d
5	3.74	22	3.1	0.82
15	11.4	18	11.1	0.97
30	22.6	16	24.5	1.08

Also given in the Table 2.1 is the detonation cell size, λ , corresponding to each hydrogen-air mixture. Based on these results, a criterion of $\lambda/d < 1$ was established for DDT to occur in such geometries (Peraldi et al., 1986). Essentially, this criterion states that in order for a mixture to undergo DDT, its detonation cell size must

2. DDT Phenomena

be smaller than the orifice inner diameter. One must keep in mind that the cell size reported is an average quantity; in reality, this value has a ± 25 percent uncertainty associated with it.

Small-scale flame acceleration tests were performed at Sandia National Laboratory in the Heated Detonation Tube (HDT) (Sherman et al., 1993). The HDT consists of a stainless steel vessel, 13.1-meters long with an inner diameter of 43.2 cm. The vessel is heated using commercial tape heaters mounted to the outside of the vessel. The maximum vessel temperature achievable using this heating system is 400K. In these tests, the HDT was filled with orifice plates with a plate spacing of roughly the inner diameter of the tube. In the series of tests relevant to this study, the orifice plates used had a blockage ratio of 0.3. Flame time-of-arrival was measured using thermocouples anchored to roughly every other obstacle. Three flush-mounted piezoelectric pressure transducers were also used to measure vessel pressure and time-of-arrival for detonation waves. Tests were performed in hydrogen-air-steam mixtures at 373K and an initial pressure of 0.1 MPa. The main objective of these tests was to determine the range of mixture composition between the flammability limit and the limit of flame propagation where the front pressure is close to the AlCC pressure. DDT limits were also reported in most cases. The tests focused mainly on the rich limits, but a limited number of tests were performed at the lean limit. The HDT results indicated that the DDT limit data could be satisfactorily correlated with $d/\lambda=1$. Results from these tests will be compared with results obtained in the present study whenever possible.

Experiments studying the effect of steam on DDT were performed at Batelle Institute (Behrens et al., 1991). The experimental apparatus consisted of a vertically mounted, closed cylindrical vessel 11 m in height and 0.8-m inner diameter within which an internal tube of length 10 m, and an inner diameter of 0.4 m is centrally positioned. The internal tube is closed at the bottom where the flame is ignited and is connected to the external vessel through the top. There are eight equally spaced orifice plates (BR=0.5) at the ignition end of the internal tube to promote flame acceleration. Most of the experiments were carried out at an initial temperature between 373K and 403K with steam fractions up to roughly 40 percent. In a typical experiment, after ignition the flame accelerates in the orifice section of the 0.4-m pipe and then decelerates when it leaves the section. In five tests, a detonation was initiated in the dome area at the top of the vessel where the flame from the internal tube emerges into the outer vessel. The authors attribute the DDT to the rapid mixing of the unburned gas with the hot products issued from the internal tube when the flame reaches the end of the internal tube. They determined that only mixtures whose cell size was less than gap dimension between the internal tube and the vessel (e.g., 0.2 m) resulted in detonations. This finding is in accord with the $\lambda/d < 1$ criteria established by the McGill experiments. As pointed out by the authors, the DDT events observed in these experiments were not the direct result of flame acceleration. The role of the initial flame acceleration on the DDT event was to generate sufficient flow so as to enhance the turbulent mixing in the dome region.

Recent experiments have been carried out by Beauvais et al. (1993) looking at the effect of initial mixture temperature on flame acceleration. The experiments were carried out in a 6-m-long tube with a diameter of 6.6 cm which could be heated to a maximum temperature of 573K. Orifice plates with blockage ratios of 0.32 and 0.7, were used in the first 3 m of the tube. The results are presented in terms of maximum flame velocity versus hydrogen mole fraction. It is not possible to deduce from the data whether or not the flame reaches steady-state conditions. At an initial temperature of 363K, they observed DDT down to a minimum hydrogen concentration of 20 percent for both blockage ratios tested. Data presented in their paper includes maximum flame velocities on the order of the CJ detonation velocity for mixtures below 20 percent hydrogen. However,

2. DDT Phenomena

they claim that in those tests since a detonation did not propagate in the smooth section of the tube, they did not consider the combustion front in the orifice section to be a detonation. For an initial temperature of 473K, DDT was observed in mixtures with a minimum hydrogen mole fraction of 12.5 and 17 percent for the 0.32 and 0.7 blockage ratio orifice plates, respectively. At 573K, they recorded only very minor flame acceleration for the 0.32 blockage ratio orifice plate configuration for all hydrogen-air mixtures tested. By rearranging the orifice plates with the first meter of the tube containing the 0.7 blockage ratio plates followed by 3 m of the 0.32 blockage ratio plates, they obtained DDT down to 12 percent hydrogen, at 553K. They also found that the use of steam as a diluent greatly reduced the likelihood of DDT.

The implication of the proposed DDT limit criterion $\lambda/d=1$, as it applies to large-scale industrial accidents, is that the larger the scale (e.g., d), the weaker the mixture which can undergo DDT. Larger scale DDT experiments were carried out at Sandia National Laboratory in the Flame Facility (Sherman et al., 1989). The Flame Facility is 30.5-m-long rectangular cross section concrete channel which is 1.83-m wide and 2.44-m high. Flame acceleration was promoted using plywood baffles placed on either side of the channel, with dimensions yielding a 0.33 blockage ratio. The Flame Facility could be operated with or without venting through the top surface. At standard temperature and pressure and with no venting, DDT was observed for a minimum hydrogen mole fraction of 15 percent, or $\lambda/d \leq 0.33$ where d is taken to be the minimum open dimension. For this mixture, DDT occurred at the end of the channel. If the Flame Facility were longer, it is possible that mixtures containing less than 15 percent hydrogen could have undergone DDT. Detonation cell size increases with decreasing hydrogen concentration and thus λ/d would approach unity.

To date, the largest scale flame acceleration tests have been performed in the RUT facility at the Kurchatov Institute (Dorofeev et al., 1996). The RUT facility consists of a reinforced concrete channel of varying cross section. Flame acceleration takes place at the ignition end which consists of a 34.6-meter-long channel which is 2.3-meters wide and 2.5-meters high. Flame acceleration is promoted by repeated concrete blocks which provide an effective blockage ratio of 0.3. In this channel section, the leanest hydrogen-air mixture at 300K that resulted in transition to detonation was 14 percent hydrogen. Transition to detonation occurred in a canyon downstream of the channel for a mixture of 12.5 percent hydrogen. It is not clear if DDT would have taken place in this leaner mixture if the channel were longer, or if the unique feature of the canyon was responsible for initiating a detonation.

The objective of the present set of experiments is to characterize the effect of mixture initial temperature on flame acceleration and more importantly on the potential for DDT. Using the cell size data for hydrogen-air-steam at elevated temperatures reported in Ciccarelli et al. (1994, 1997), we will determine if the $\lambda/d \leq 1$ criterion applies at elevated initial temperatures up to 650K. Unlike in the previous experiments carried out by Beauvais et al. (1993), the entire length of the test vessel will be filled with orifice plates in order to allow the flames to achieve a steady-state velocity.

2. DDT Phenomena

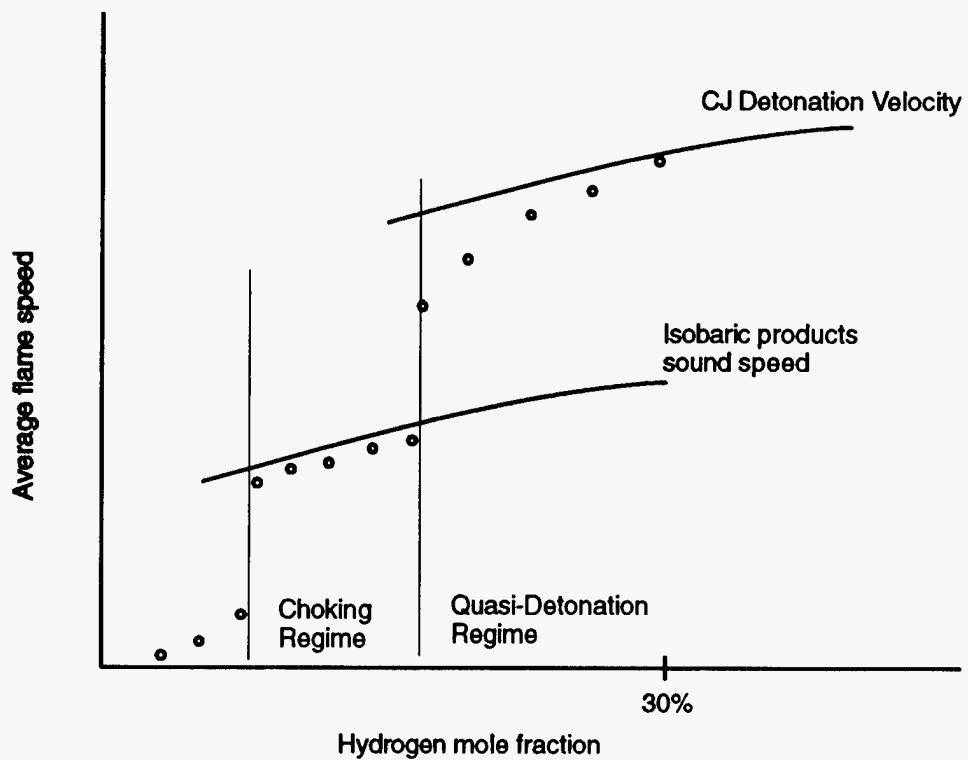


Figure 2.1 Schematic showing the steady-state flame propagation regimes

3. EXPERIMENTAL DETAILS

The DDT experiments were carried out in the BNL High-Temperature Combustion Facility (HTCF) which is a 27-cm-inner diameter, 21.3-m-long heated detonation vessel. The vessel is made up of seven equal-length flanged sections, as shown in Figure 3.1. A detailed description of the HTCF detonation vessel, the gas handling system, and other auxiliary equipment can be found in Ciccarelli et al. (1997). Flame acceleration is promoted by an array of obstacles placed inside the entire length of the detonation vessel. The obstacles consist of orifice plates which are 1.9-cm thick, with a 27.3-cm outer and 20.6-cm inner diameter. One can define an orifice blockage ratio, BR, as the area of the orifice opening (πd^2) to the cross-sectional area of the vessel (πD^2), or $BR = (D^2 - d^2)/D^2 = 1 - (d/D)^2$. For a 20.6 cm orifice opening and a 27.3 cm vessel inner-diameter, this yields a blockage ratio of 0.43. The obstacle spacing is one tube diameter (i.e., 27 cm). These two parameters, blockage ratio and orifice plate spacing, are similar to those used in the McGill experiments, thereby making it possible for a direct comparison of their results with the present results. It should be noted that the values of both these parameters were found by the McGill research to provide the optimum configuration for flame acceleration and DDT. The orifice spacing is maintained by fastening the orifice plates to threaded rods with nuts on either side of each plate. There are six equally spaced, circumferentially mounted, 1.9-cm diameter threaded rods as shown in Figure 3.2. The threaded rods are anchored to the vessel at vessel flange locations. That is, the threaded rods are fixed at one end of a vessel section to special orifice plates, that have outer diameters larger than the vessel inner diameter, thus allowing these plates to be sandwiched between each pair of vessel flanges. Mounting arrangements for the orifice plates account for the thermal expansion of the threaded rods during heating of the vessel.

A flame is ignited in the test vessel by a standard diesel engine glow plug mounted centrally on one of the vessel end plates. The glow plug is powered through a 120/12 VAC step-down transformer. Depending on the initial mixture temperature, ignition occurs between 10 and 20 seconds after the power is first applied to the glow plug.

The detonation vessel is equipped with instrumentation ports located every 61 cm down the length of the tube. The combustion front velocity is measured using ionization probes, photo diode detectors, and fast response thermocouples. The best time-of-arrival data was obtained from the photo diode detectors. For slow propagating flames, the intensity of light emitted from the flame is insufficient to obtain a signal from the photo diodes, in which case the flame velocity is determined based on thermocouple signals. Combustion front pressure is measured using one piezoelectric pressure transducer located near the end of the vessel. The signals from the photo diodes, ionization probes, and pressure transducers are recorded on two digital LeCroy oscilloscopes, and the thermocouple signals are recorded on a slower PC-based data acquisition system. The data acquisition card used was a Strawberry Tree ACPC-16 with a maximum sampling rate of 1.3 kHz.

Gas samples are taken from the vessel just before ignition to compare the measured hydrogen concentration with the expected hydrogen concentration. The gas samples are analyzed in-house using a Carle gas chromatograph. In all the tests performed, the measured hydrogen concentration was within 1-2 percent of the expected concentration.

3. Experimental Details



Figure 3.1 Photograph of the HTCF Detonation Vessel

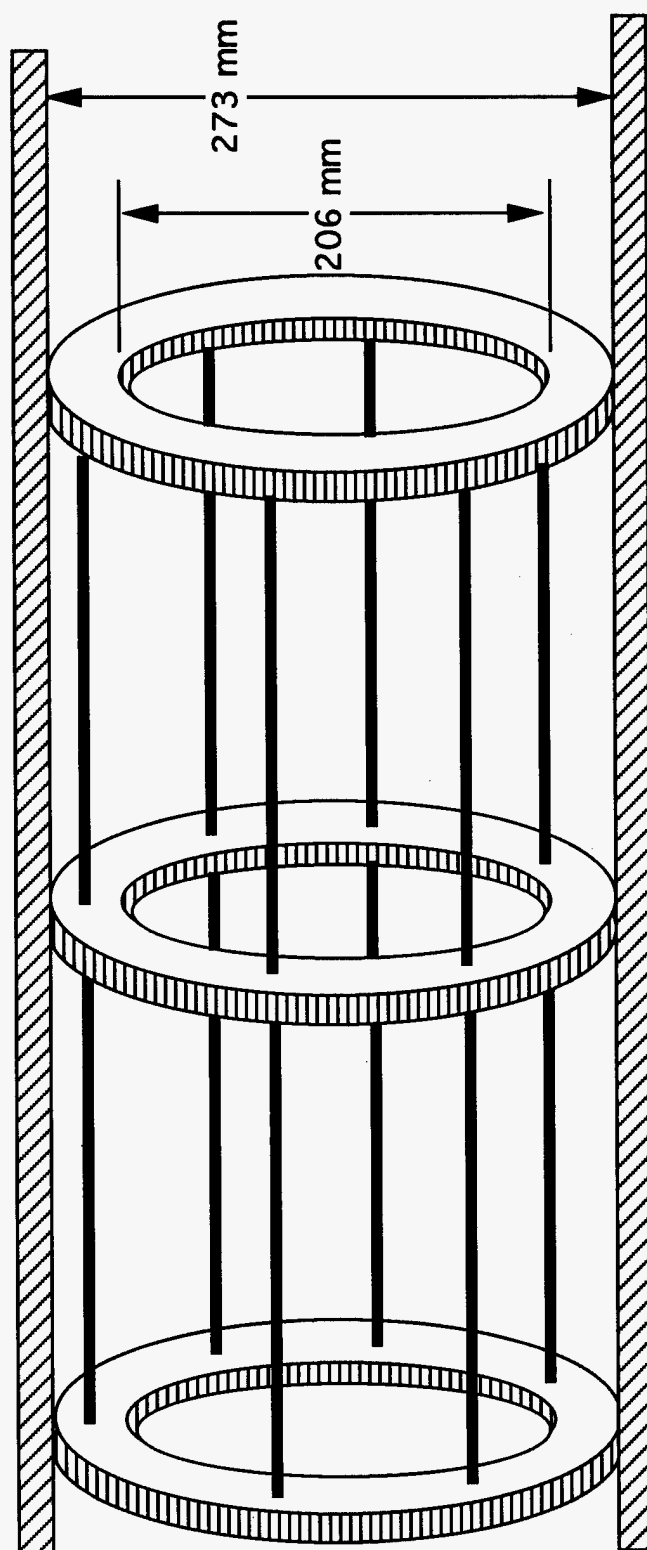


Figure 3.2 Schematic of Orifice Plate Geometry and Dimensions

4. EXPERIMENTAL RESULTS

As described in the Introduction, flame propagation in an obstacle-laden (e.g., orifice plates) tube consists of an initial acceleration phase followed by a steady-state phase where the flame globally attains a constant velocity. However, even in this so-called steady-state region, local flame propagation from one orifice plate to the next is quite transient due to gasdynamic effects caused by flow restriction through the orifice. In this study, we are interested in the global flame propagation mode and not so much in the details of the local phenomenon. The axial spacing of the time-of-arrival instrumentation (e.g., photo diodes), is therefore large, typically 3.05 m. In the following sections, flame acceleration and final steady-state velocities are reported as a function of the hydrogen-air-steam composition and mixture initial temperature. All tests were performed at an initial pressure of 0.1 MPa. A summary of the initial conditions and the experimental results are provided in Appendix A.

4.1 Flame Propagation Regimes

Plotted in Figure 4.1 is the flame front velocity versus axial distance for three different hydrogen-air mixtures at 300K. These three experiments characterize the spectrum of flame propagation modes observed in the current study. The various flame propagation regimes have been classified as: (1) detonation¹, (2) choking, and (3) slow deflagrations. These three flame propagation regimes are observed irrespective of the initial mixture temperature and steam dilution.

4.1.1 Detonation Regime

In Figure 4.1, the variation in flame speed with distance, or flame trajectory, in the 16 percent hydrogen mixture is typical for steady-state flame propagation in the detonation regime. The flame acceleration takes place in the first six meters followed by a relatively steady propagation at a velocity of 1130 m/s. The variation in the measured velocity between the 6-meter station and the end of the vessel is 22 m/s. The average velocity along this length of the vessel is roughly 27 percent below the theoretical Chapman-Jouget velocity for this mixture. There is a slight overshoot in the velocity before reaching steady state. This overshoot is typical of a DDT event, because the detonation is initiated in a region ahead of the flame where the gas has been pre-compressed by the accelerating flame. In this region, the cell size is smaller than at the 0.1 MPa test pressure, hence the losses are less, and, therefore, the detonation velocity more closely matches the CJ velocity which is not sensitive to the mixture pressure. This velocity overshoot is observed, to various degrees, in all the experiments in the detonation regime. The actual maximum velocity overshoot is probably more than that indicated in the figure because the large spacing between time-of-arrival instrumentation only yields velocities averaged over three meters.

The pressure time history measured near the end of the 21.3-meter-long vessel (e.g., 17.4 meters from ignition end) for the 16 percent run is shown in Figure 4.2a. The peak overpressure of the first pulse is about 0.93 MPa. Behind the initial pressure rise, the average pressure decays monotonically, which is typical in the

¹The detonation regime observed in this study is similar to the quasi-detonation regime reported in Guirao et al. (1989).

4. Experimental Results

expansion fan which exists behind the detonation front (Nettleton, 1987). The large pressure oscillations after the initial pressure rise are due to a combination of the shock reflections caused by the periodic orifice plates and the pressure oscillations associated with the cellular structure of the detonation wave.

4.1.2 Choking Regime

The variation in flame speed with distance is shown in Figure 4.1 for the 12 percent hydrogen mixture is typical for flame propagation in the choking regime. As in the 16 percent hydrogen case, the flame propagates at a relatively steady velocity after an initial acceleration phase in the first six meters of travel. Although not very evident in this test, there is a velocity overshoot that typically follows the initial flame acceleration phase. The average velocity for the flame after six meters is 644 m/s with a standard deviation of 8 m/s. This matches very closely the speed of sound in the products for this mixture.

The pressure-time history recorded at an axial distance of 17.4 m from the ignition source is given in Figure 4.2b. This pressure profile is very different in structure from the one corresponding to the detonation wave, shown in Figure 4.2a. The initial pressure rise up to 0.23 MPa is followed by a pressure plateau which lasts about 0.3 ms ending in a second abrupt pressure rise. This second pressure rise is due to the reflected wave from the orifice plate located just 6.4 cm ahead of the pressure transducer. Taking the shock overpressure reading from Figure 4.2b (e.g., 0.23 MPa), and using the normal shock tables, yields a shock Mach number of 1.1 and a shock velocity of 405 m/s. The speed of sound and particle velocity behind such a weak shock is 418 m/s and 24 m/s, respectively. Assuming that the reflected wave, which for this choking regime is also relatively weak, propagates at the local speed of sound, we get a net wave velocity of 394 m/s, which is not much different from the incident shock speed of 405 m/s. Therefore, the transit time between the pressure transducer and the orifice plate for both the incident and reflected shock wave is about 0.16 ms based on a transit distance of 6.4 cm. This yields a total round-trip time of 0.32 ms. This time corresponds very closely to the time between the first and second pressure rises in Figure 4.2b. The obvious difference in the pressure profiles obtained for the detonation wave shown in Figure 4.2a, and for the flame propagation in the choking regime shown in Figure 4.2b can be used in conjunction with the average propagation velocity to identify the propagation regime. The pressure signal is especially useful for those mixtures where there is no abrupt change in the average velocities recorded between the choking and the detonation regime.

The constant pressure after the initial pressure rise indicates that the shock is propagating at a constant velocity. For a Mach 1.1 incident shock wave, the temperature rise across the shock is only 20K which is too small to initiate any chemical reactions in the mixture. Since there is no chemical energy release by way of adiabatic compression of the test mixture directly behind the shock wave, the only way the shock can keep from decaying is through the piston action of the trailing flame. Therefore, the structure of the front in the choking regime consists of a precursor shock driven by a deflagration, and since the deflagration propagates at the speed of sound in the products, it is considered a CJ deflagration.

4.1.3 Slow Deflagration

Any light emitted from the slow flames produced in these mixtures was insufficient for detection by the photo diodes. As a result, flame velocity measurements could only be derived in the first half of the tube, which was equipped with four thermocouples. In Figure 4.1, for the 10 percent hydrogen mixture, the flame initially

4. Experimental Results

accelerates to a maximum velocity of about 250 m/s and then decelerates to roughly 100 m/s. For leaner mixtures (not shown), the flame velocity increases very slowly reaching 100 m/s by mid vessel. Due to the lack of instrumentation in the second half of the tube, it is not clear from this figure whether or not the flame velocity achieves a constant velocity or continuously decays with distance. In tests with lean mixtures but at higher initial temperatures, the flame velocity was observed to reach a maximum and then decelerate to very low velocities on the order of meters per second.

In experiments carried out at McGill with very lean mixtures near the flammability limit, flames were observed to propagate for some distance and then self-extinguish (Lee et al., 1984). This type of behavior was found to be typical for mixtures with very low burning velocities, such as methane-air. This so-called "flame quenching" was not observed in the present experiments in hydrogen-air-steam mixtures at any of the initial temperatures tested. This is probably due to the relatively high burning velocity associated with these more sensitive mixtures. At 300K, the flammability limit was found to be between 8 and 8.5 percent hydrogen. This flammability limit is based on the absence of any temperature rise being detected in the first thermocouple located at roughly one meter from the point of ignition. This value is closer to the upward flammability limit at 300K of 9 percent hydrogen reported by Kumar (1985) using a standard smooth tube than to the reported horizontal limit of 6.5 percent hydrogen. The higher limit obtained in the present experiments could be due to flame stretch induced by the obstacles on the flame or perhaps quenching caused by the gas dynamic effects of the flow through the orifice plates.

4.2 Flame Propagation Regimes at 300K

Shown in Figure 4.3 is a plot of the flame velocity as a function of the mixture hydrogen mole fraction. For each test resulted in flame propagating either the choking or detonation regimes, the average velocity (shown as an open circle) is based on measurements obtained in the last half of the vessel. The vertical bar indicates the standard deviation in the velocity measurements used to obtain the average velocity for each test. Also shown in the plot are the theoretical curves for the mixture CJ detonation velocity and the isobaric sound speed in the combustion products. The open squares represent the *maximum* velocity measured for mixtures in the slow deflagration regime.

No abrupt change in the average propagation velocity as a function of hydrogen concentration is noted in Figure 4.3 that would clearly indicate a separation between the choking and the detonation regimes. The figure shows a somewhat continuous decrease in the average velocity from very close to the CJ detonation velocity for a 30 percent hydrogen mixture down to just below the isobaric product sound speed for a 13 percent hydrogen mixture. Recall in the detonation regime, the detonation wave propagates at a sub-CJ detonation velocity due to momentum and heat losses. The amount of energy lost from the reaction zone depends on the length of the reaction zone, which is proportional to the detonation cell size for the mixture. Since the detonation cell size increases with decreasing hydrogen concentration, one would expect the average propagation velocity relative to the CJ detonation velocity to decrease with decreasing hydrogen concentration, as is generally observed in Figure 4.3. At 15 percent hydrogen, the measured velocity is 31 percent below the CJ detonation velocity, and at 30 percent hydrogen, which has the smallest cell size, the velocity deficit is only 3 percent. The data does seem to indicate a noticeable, but slight, change in the velocity trend between 14 and 15 percent hydrogen, suggesting a demarcation from one regime to another. However, for flame propagation in the choking regime, the average velocity is typically below the isobaric

4. Experimental Results

speed of sound in the products which is not the case for the 14 percent hydrogen mixture. The average velocity measurements indicate that the lean limit for the choking regime is at 11 percent hydrogen. Tests conducted at this condition with hydrogen mole fractions between 8.5 and 10 percent showed that the maximum flame velocity shown in Figure 4.3 is achieved in the first three meters, followed by a decrease in velocity over the remainder of the vessel.

Based on these factors, it appears that the DDT limit should lie somewhere between 13 and 15 percent hydrogen. To help narrow the gap, we used the measured pressure signals. Indications of the DDT limit can be obtained by examining the measured shock overpressure versus hydrogen concentration, as shown in Figure 4.4. Typically, pressure profiles are very difficult to interpret quantitatively because of the large oscillations following the initial pressure rise. For detonations, the measured detonation pressures (e.g., Figure 4.4) are obtained by averaging across the oscillations. Typically, the actual magnitude of the oscillations can be quite large compared to the magnitude of the recorded signal. The lines in Figure 4.4 represent the theoretical CJ detonation pressure and the AICC pressure. The plot clearly shows an abrupt change in the measured shock pressure at 15 percent hydrogen. For mixtures of 15 percent and higher, the pressure is scattered about the CJ detonation pressure, and for mixtures below 15 percent hydrogen, the pressures are below the AICC pressure. Furthermore, the pressure profile for the mixtures with less than 15 percent hydrogen exhibit a rapid initial pressure rise followed by a pressure plateau similar to the one depicted in Figure 4.2b. Note, the peak overpressures shown in Figure 4.4 correspond to the initial pressure rise from the advancing front and not the reflected pressure. Therefore, based on the measured overpressures, 15 percent hydrogen is considered to be the DDT limit for the hydrogen-air mixtures at 300K. For mixtures below 11 percent hydrogen, there was no discernible pressure transient detected with the passage of the flame, largely due to the relatively low sensitivity of the pressure transducers (e.g. 5 mV/psi).

Taking 15 percent hydrogen to be the lean limit for DDT to occur, we can check the $d/\lambda = 1$ DDT criterion obtained in the McGill experiments in a similar orifice filled tube. The cell size for a 15 percent hydrogen mixture at 300K and 0.1 MPa is about 21.8 cm (Ciccarelli et al., 1997), and the inner diameter of the rings is 20.6 cm. Therefore, the ratio d/λ equals 1.0, which is in excellent agreement with the McGill experiments.

4.3 Flame Propagation Regimes at 500K

Figure 4.5 is a plot of flame velocity versus distance for three different hydrogen-air mixtures at 500K and 0.1 MPa. The flame trajectory in the 20 percent hydrogen mixture is an example of propagation in the detonation regime where DDT occurs close to the point of ignition. The average velocity over the last half of the tube is 1564 m/sec, about 8 percent below the theoretical CJ detonation velocity for this mixture. This trajectory is similar to the one depicted in Figure 4.1 for the 16 percent hydrogen mixture at 300K. In the 12 percent hydrogen mixture, the final propagation mode is also a detonation; however, the detonation requires a longer distance to develop. The run-up distance, defined as the distance the flame propagates before DDT, is about 10 meters for this mixture. As a result of the longer run-up distance and the velocity overshoot, there is very little length of vessel remaining for the detonation to stabilize. In this case, only the last two velocities can be considered when calculating an average flame velocity. The flame trajectory shown in Figure 4.5 for the 11 percent hydrogen mixture is an example of flame propagation in the choking regime. There is an overshoot in the flame velocity where the peak is above the speed of sound (700 m/s) of the product gases. In this case, the flame also achieves a steady-state velocity but only very close to the end of the vessel.

4. Experimental Results

The average flame velocity data obtained for hydrogen-air mixtures at 500K is given in Figure 4.6. Here, there is a clear demarcation in the trend of the experimentally measure average flame velocity data occurring between 11 and 12 percent hydrogen. The DDT limit can be assumed to be 12 percent hydrogen. For mixtures between 8 and 11 percent hydrogen, the data follows very closely the theoretical isobaric sound speed of the product gases. It is also evident that the experimental average velocity data lies closer to the theoretical CJ detonation velocity compared to that observed at 300K, in Figure 4.3. For example, for a 15 percent hydrogen mixture, the measured velocity is 15 percent below the CJ detonation velocity, and at 30 percent hydrogen, the velocity deficit is only 2 percent. This can be attributable to the decrease in cell size (i.e., reaction zone length) with increased temperature (Ciccarelli et al., 1997) resulting in less frictional/heat transfer losses. The flammability limit at this temperature was found to be between 7 and 7.5 percent hydrogen which is lower than the 8.5 flammability limit at 300K. The lowering of the flammability limits with increased temperature is consistent with data in the literature (Kumar, 1985). For the 7.5 percent hydrogen mixture, the flame propagation velocity was measured to be below 2 m/s throughout the first half of the vessel where the thermocouples were located. This velocity is just above the laminar burning velocity for this mixture. Note for such a slow moving flame, the products cool considerably and thus the apparent velocity can be close to the laminar burning velocity for the mixture.

Shown in Figure 4.7 is the measured shock pressure as a function of hydrogen mole fraction for hydrogen-air mixtures at 500K and 0.1 MPa. Mixtures of 12 percent or higher show measured pressures larger than the corresponding AICC pressure but lower than the detonation pressure. Mixtures with less than 12 percent hydrogen exhibit pressures consistently below the AICC pressure. This transition in the measured overpressures at 12 percent hydrogen is consistent with the DDT limit observed from the average velocities in Figure 4.6. The cell size for a 12 percent hydrogen mixture at 500K and 0.1 MPa is about 13.5 cm (Ciccarelli et al., 1997) which yields a value of 1.5 for the ratio d/λ . The value of this ratio can be considered as satisfying the $d/\lambda = 1$ criterion for DDT transition, considering of course the uncertainty in the experimentally measured detonation cell size,

The results obtained at 500K can be compared to those obtained in the HDT test facility (Sherman et al., 1993). With the HDT filled with orifice plates with a BR of 0.3, a series of tests were performed at 373K and 0.1 MPa. When comparing results, one must keep in mind that the HDT has a larger inner diameter than the HTCF, and the blockage ratio in the two studies are different. Tests in the HDT reported a DDT limit at 13 percent hydrogen. In the present study, the DDT limit was found to be 15 percent hydrogen at 300K and 12 percent hydrogen at 500K; therefore, the HDT results obtained at 373K fall in the range obtained in the present studies. The so-called "flame acceleration" limit in the HDT was found to be 9 percent hydrogen at 373K. The flame acceleration limit was defined by Sherman et al. (1993) as the limiting mixture in which the observed peak pressure first exceeds the AICC pressure. Since a flame front pressure on the order of the AICC pressure is typical for steady-state flame propagation in the choking regime, the flame acceleration limit reported for the HDT can be compared with the choking limit observed in the present experiments. The 9 percent hydrogen limit observed in the HDT at 373K lies in the range of the observed choking limit in the present study, i.e., 8 and 11 percent hydrogen at 500K and 300K, respectively. The above agreement between the two experiments provides a degree of confidence in the results reported in the next section.

4.4 Flame Propagation Regimes at 650K

The flame trajectory for several hydrogen-air mixtures at 650K and 0.1 MPa is shown in Figure 4.8, which shows that DDT occurred in 11, 12, and 17.5 percent hydrogen mixtures. It is clear from this figure that the run-up distance increases with decreasing hydrogen concentration. For example, DDT occurs in the last vessel section for the 11 percent hydrogen mixture. In the DDT experiments conducted at 300K and 500K, typically there was an overshoot in the velocity at the point of DDT followed by a relatively quick (e.g., 5 meters) decay to a steady-state velocity. The results in Figure 4.8 indicate that achieving a detonation at 650K requires a much longer distance for the advancing flame to reach steady-state conditions. For example, for the 17.5 percent hydrogen mixture, DDT occurs after about six meters of propagation, and from that distance to the end of the vessel, the detonation velocity consistently decreases. A similar type of behavior is observed in the 12 percent hydrogen case shown in Figure 4.8. It is interesting to note that dropping the hydrogen mole fraction from 11 to 10.5 percent, a difference of only 0.5 percent hydrogen, results in a benign burn. In the 10.5 percent hydrogen mixture, the flame accelerates to a maximum velocity of about 100 m/s and then decays to roughly the laminar burning velocity.

It is difficult to assign an average velocity to any of the velocity profiles shown in Figure 4.8 since the detonation never achieves steady-state conditions within the length of the vessel. This is especially true for the leaner mixtures where the run-up distances can be quite large. Therefore, in Figure 4.9, the last velocity measurement taken at the end of the vessel (between 16.7 and 19.8 meters) in each experiment carried out at 650K and 0.1 MPa is shown as a function of the hydrogen mole fraction. Note these are not average velocities and thus no error bars are shown to depict the standard deviation. The measured detonation velocity decreases smoothly with decreasing hydrogen mole fraction just below the theoretical CJ detonation velocity. The minimum hydrogen concentration resulting in a DDT is 11 percent hydrogen. As indicated above, for the 10.5 percent hydrogen mixture, the maximum flame velocity is only about 100 m/s. As a result, no flame propagation in the choking regime was observed. The 11 and 10.5 percent hydrogen tests were repeated several times to verify the observed behavior. In the three tests run with 11 percent hydrogen, the flame accelerated through the entire vessel reaching a maximum at the end of the vessel. Therefore, the high detonation velocities, shown in Figure 4.9, are the result of DDT occurring at the end of the vessel where the last velocity measurement is taken. Recall, the overshoot in the velocity is caused by the initial overdrive of the detonation resulting from the initiation process and also due to the fact that the gases ahead of the flame front are at a higher pressurized temperature than the initial conditions. For this test series, the flammability limit at 650K was determined to be between 5 and 5.5 percent hydrogen.

In these tests, a pressure transducer was located at 17.4 meters, in between the two photo diodes used to obtain the velocities plotted in Figure 4.9. The peak shock pressure measured at this location is shown in Figure 4.10 as a function of hydrogen mole fraction. All the pressures measured, except for one at 11 percent hydrogen, are consistent with detonations. For the tests runs with 11 and 12 percent hydrogen mixtures, the measured pressures are high relative to the theoretical CJ pressures, when compared to the shock pressures for the richer mixtures which are very close to the CJ detonation pressure. The measured high pressures are due to the proximity of the pressure transducer to the point of DDT, where the detonation is overdriven. As the detonation propagates away from the point of DDT, the detonation velocity approaches the CJ detonation velocity for the mixture and the peak detonation pressure decays correspondingly. As a result, the pressure measured by the transducer depends on the distance between the transducer and the location of DDT. Since

4. Experimental Results

the run-up distance, for a given mixture varies from test to test, one would expect to see a scatter in the measured shock pressures. This scatter is evident in the pressures obtained in the 11 and 12 percent hydrogen mixtures shown in Figure 4.10. Two data points in Figure 4.10, both of them corresponding to an 11 percent hydrogen mixture, are noteworthy. These two points emphasize the effect of DDT location on the shock pressure measured. In one of these tests with an 11 percent hydrogen mixture, DDT occurred just ahead of the transducer, and as a result, the peak pressure is very high, almost 30 percent higher than the CJ detonation pressure for the test mixture. In the other test, DDT occurred after the pressure transducer, and as a result, the overpressure measured is typical of flame propagation in the choking regime, with a shock pressure of 0.28 MPa, which is just over the AICC pressure. This is roughly half the CJ detonation pressure for the mixture. Using the normal shock tables, the post-shock temperature for a 0.28 MPa shock wave is 910K. If the detonation is initiated in the compressed gas region between the flame and the leading shock wave, the detonation pressure would be larger than the CJ detonation pressure in the test mixture. The theoretical CJ detonation pressure is 0.98 MPa, or roughly 2 times the CJ detonation pressure at an initial pressure of 0.1 MPa and temperature of 650K. Therefore, the elevated pressures measured in the other two tests conducted in an 11 percent hydrogen mixture shown in Figure 4.10 are compatible with a detonation occurring in the compressed gas behind the leading shock wave that had been generated by the advancing flame front.

Both the detonation velocity and overpressure data presented show that 11 percent is the minimum hydrogen composition which results in a DDT occurring within the tube. The cell size for an 11 percent hydrogen mixture at 650K and 0.1 MPa is about 3.7 cm (Ciccarelli et al., 1997). This yields a value of 5.5 for the ratio d/λ , which means that at the limit about five detonation cells or more can pass through the inner diameter of an orifice plate. Even if a conservative estimate of ± 50 percent is taken for the uncertainty in the cell size measurements, the ratio becomes $3.7 < d/\lambda < 11.1$. Clearly the observed minimum hydrogen composition of 11 percent for DDT at 650K does not meet the DDT criterion of $d/\lambda = 1$, which has been shown to be applicable for the data obtained at 300K and 500K.

One of the difficulties in analyzing the data at 650K is that the detonation does not achieve steady-state conditions within the length of the vessel. The main reason is the long run-up distances at this temperature which depend on the initial flame acceleration process. Steady-state detonations could be obtained for these conditions if the run-up distances are decreased, possibly by somehow increasing the initial flame acceleration rate. Figure 4.11 is a plot of the initial acceleration phase for an 11 percent hydrogen mixture at various initial temperatures. This figure shows that flame acceleration in the first six meters of travel is highest at an initial mixture temperature of 300K and lowest at 650K. This observation of increasing flame acceleration with decreasing initial temperature can be exploited for reducing run-up distances by pre-accelerating the flame before it enters the test mixture at 650K. This was accomplished by testing in an environment where the first two vessels (e.g., 6.1 meters) were maintained at 400K temperature while the remaining vessel sections were heated to the test temperature of 650K. These experiments are not meant to simulate any conditions which occur during an accident in a nuclear power plant, the objective is to demonstrate that the experimentally measured DDT limit is not a fundamental detonation property.

The average velocities measured during tests conducted at 650K and 0.1 MPa, but with the first 6.1 meters of vessel at roughly 400K, are given in Figure 4.12. DDT did not occur in the cold section of the tube. In general, DDT occurred within the range of 7.6 and 10.1 meters from the point of ignition, which is just outside

4. Experimental Results

the cold section, leaving sufficient distance to the end of the vessel for the detonation to achieve steady conditions. The error bars denote the standard deviation in the velocity measurements, which are very small for these tests. The data points for the 10 percent hydrogen mixtures do not have error bars since DDT occurred at the end of the vessel. The average velocities shown in Figure 4.12 are slightly higher than the terminal velocities obtained when the entire length of the vessel is at 650K, as shown in Figure 4.9. This would indicate that in those tests where the entire vessel was heated to 650K, the detonation velocity would have eventually decayed to the CJ velocity if the vessel were longer. With the first 6.1 meters of the vessel at 400K, DDT occurred in hydrogen-air mixture concentrations as low as 9.5 percent hydrogen. Therefore, mixtures of 9.5 and 10 percent hydrogen which did not transition to a detonation when the vessel was completely heated now show that a DDT had occurred. The cell size for a 9.5 percent hydrogen in air mixture at 650K is 4.6 cm (Ciccarelli, 1997). This yields a value of 4.5 for d/λ , which is still well above the DDT criterion found to be valid for the tests at 300K and 500K. The implications of these results will be discussed later in the report in Section 5.2.

4.5 Flame Propagation Regimes in Hydrogen-Air-Steam Mixtures

The influence of steam dilution on flame acceleration and DDT phenomenon was studied in hydrogen-air mixtures at initial temperatures of 400K, 500K, and 650K. In these tests, the steam dilution fraction was held constant and the ratio of the hydrogen to air mole fraction was varied (i.e., hydrogen mole fraction on a dry basis). In this way, one can obtain a minimum hydrogen composition resulting in DDT for a given steam dilution and initial temperature. Tests were conducted at two distinct steam dilutions, namely 10 and 25 percent.

For the 10 percent steam dilution, the average flame velocities measured in hydrogen-air mixtures at 400K and 0.1 MPa are shown in Figure 4.13. The flame achieved steady-state conditions well before the end of the vessel for all the cases tested. The trend in the experimental data was found to be similar to the previous trends shown without steam dilution. The DDT limit and the choking limit were found to be 18 and 12 percent hydrogen, respectively. The flammability limit was found to be between 9 and 9.5 percent hydrogen. The cell size for an 18 percent hydrogen in air mixture with 10 percent steam dilution at 400K is 30.5 cm (Ciccarelli et al., 1997), yielding a value of d/λ equal to 0.7. This is in reasonably good agreement with the DDT criterion observed in hydrogen-air mixtures without steam at 300K and 500K. The DDT limit obtained from the HDT for 18 percent hydrogen in air mixtures at 373K was between 8 and 9 percent steam dilution (Sherman et al., 1993). The inner diameter of the 0.3 BR orifice plates employed in the HDT was 35.6 cm. If we assume that the cell size for this mixture is similar to the 18 percent hydrogen in air mixture with 10 percent steam dilution at 400K, this yields a value of d/λ equal to 1.2. Therefore, the experimentally observed values of d/λ at the DDT limit, obtained from the present tests and the HDT tests bracket the $d/\lambda=1$ criterion (e.g., $0.7 < d/\lambda < 1.2$).

Shown in Figure 4.14 are the average flame velocities for hydrogen-air mixtures with 25 percent steam dilution at 500K and 0.1 MPa. For a 24 percent hydrogen mixture, the flame was observed to propagate both in the choking and detonation modes. Therefore, one can assume that 24 percent hydrogen is the DDT limit based on this transitional behavior. Cell size data for this limiting condition is not available from previous studies. However, an estimate of the cell size was obtained by using the ZND model to calculate a chemical reaction zone length and multiplying this length by a proportionality constant of 25 (Ciccarelli et al., 1997). The calculated reaction zone length for this mixture is 1.24 cm which, with the above proportionality constant,

4. Experimental Results

gives a cell size of 31.1 cm. Based on this calculated cell size, d/λ is 1.5. For this test series, the choking and flammability limits were determined to be 14 and 11 percent hydrogen, respectively.

Tests were also performed with hydrogen-air mixtures diluted with 25 percent steam at 650K and 0.1 MPa. For all the hydrogen-air mixtures tested, flame acceleration terminated in a peak velocity followed by a slow decay in the flame velocity. As was the case in the dry hydrogen-air mixtures at 650K, the flame never achieved steady-state conditions by the end of the vessel. Shown in Figure 4.15 is the last velocity measurement in the vessel as a function of hydrogen mole fraction. Flame propagation in the choking regime was observed in mixtures between 16 and 18 percent hydrogen. This differs from the observation in the dry hydrogen-air mixtures at 650K where no choking regime was observed. Figure 4.16 shows that for a 18 percent hydrogen mixture the flame accelerated to a peak velocity in excess of the CJ detonation velocity and then decayed to a velocity just below the speed of sound in the combustion products. A plausible interpretation is DDT followed by detonation propagation failure. Tests at this condition were repeated several times in order to determine the repeatability of this phenomenon. In two other tests performed with 18 percent hydrogen peak velocities on the order of 1250 m/s were measured. Although this velocity is well below the 1650 m/s peak velocity in Figure 4.16, it is still about 450 m/s above the speed of sound in the products. It is difficult to determine, based solely on the velocity measurements, whether or not DDT had occurred under these test conditions. The final velocity for the 16 percent hydrogen mixture in Figure 4.15 is above the speed of sound in the products because the peak velocity occurred close to the end of the tube. Based on the velocity measurement presented, it appears that the DDT limit for 25 percent steam diluted hydrogen-air mixtures at 650K is 19 percent hydrogen.

The tests shown in Figure 4.15 were repeated with the first 6.1 meters of the vessel maintained at a temperature of 400K. The results from these tests are shown in Figure 4.17 as the average velocity versus hydrogen mole fraction. The DDT limit remains the same as that observed in Figure 4.15; however, even with the colder initial section, a steady-state velocity is not obtained by the end of the vessel. Using the ZND model, the reaction zone length was calculated to be 0.49 cm. Using a proportionality constant of 50 (Ciccarelli et al., 1997) yields a calculated cell size for this mixture of 24.3 cm. This yields a value of 1.2 for d/λ , which is in good agreement with the DDT criterion. The choking limit was determined to be 16 percent hydrogen. The average velocity observed in the choking regime is just below the speed of sound in the products which is in line with the previous results. A rough estimate of the flammability limit was found to be between 4.5 and 8 percent hydrogen.

4.6 Detonation Run-Up Distance

The detonation run-up distance is defined as the flame propagation distance from the ignition source to where transition to detonation occurs. Experimentally, this run-up distance restricted the length of tube over which the detonation could stabilize after DDT. However, this parameter is also very important in assessing the geometric length scales required for a flame to accelerate and transit to detonation. DDT is a local phenomenon which occurs on a scale of the order of the detonation cell size (e.g., centimeters). The run-up distance is determined by identifying the location in the tube where DDT occurs. The most direct and precise method to identify the location of DDT is to use a smoked foil to determine the location in the tube where detonation cells first appear. However, experimentally, this approach is not practical. The DDT event is preceded by a monotonic increase in the flame velocity followed by a monotonic decay in the detonation

4. Experimental Results

velocity approaching the mixture CJ detonation velocity. Therefore, the simplest approach for identifying the location of DDT is by identifying the location in the tube where the peak flame velocity is measured. Using this approach, the accuracy of the measurement of the run-up distance is governed by the spacial resolution of the time-of-arrival instrumentation.

The measured run-up distance in the hydrogen-air mixtures at 300K, 500K, and 650K are shown in Figure 4.18. In all cases, the photo diodes were used as the time-of-arrival instruments. The symbols in Figure 4.18 identify the midpoint between the photo diode locations where the peak flame velocity was measured for each run. The error bars show the distance between the two bounding photo diodes, which in general, is on the order of three meters. Figure 4.18 indicates that both the hydrogen mole fraction and the initial mixture temperature influence the run-up distance. It is apparent from the figure that the hydrogen mole fraction is the more important of the two parameters, especially for hydrogen mole fractions below 15 percent. The DDT limit at 300K is 15 percent hydrogen; as a result, to within experimental accuracy, the run-up distance is unaffected by hydrogen mole fraction. Note the data point for 11 percent hydrogen at 650K includes three runs.

4. Experimental Results

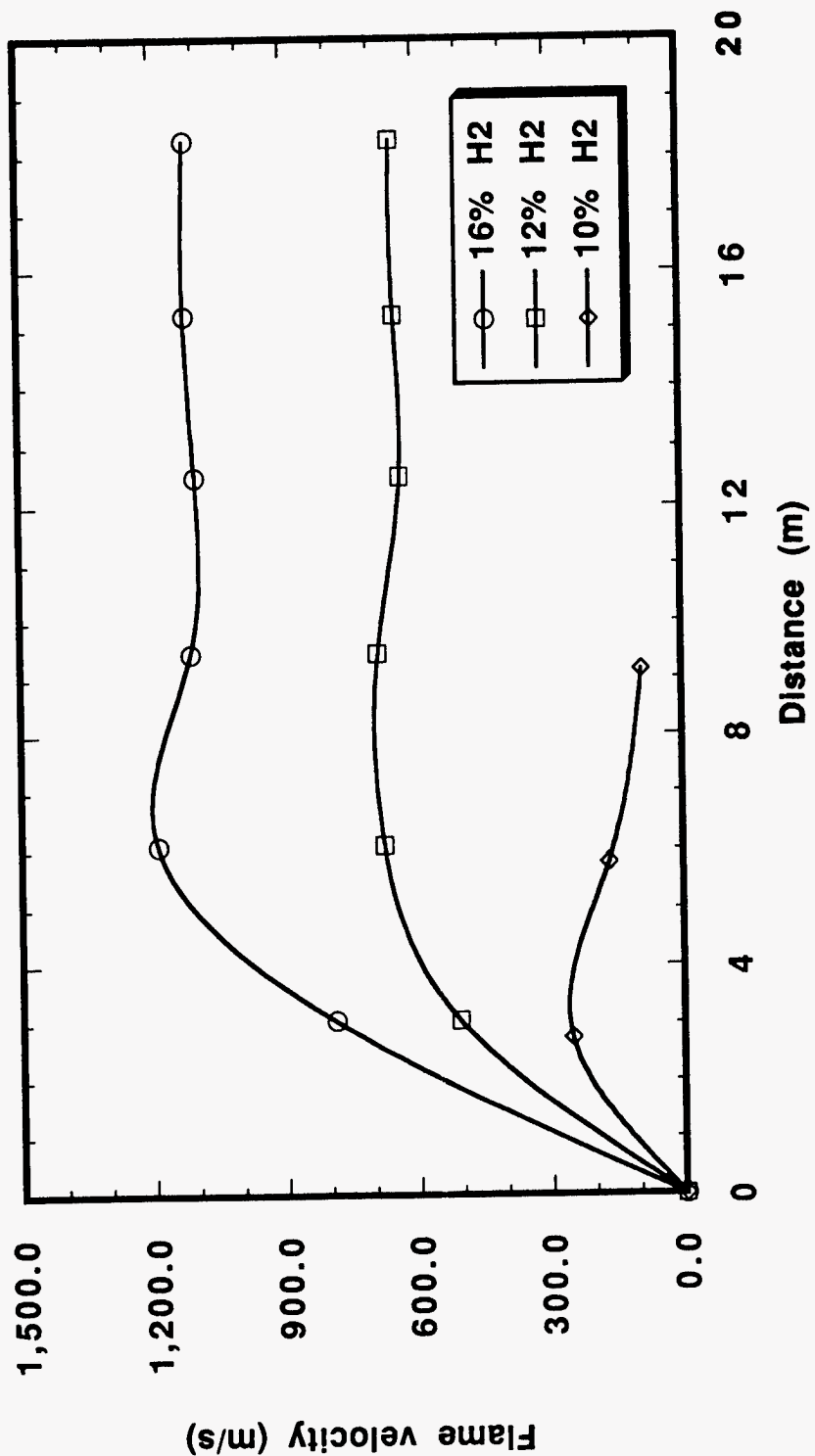


Figure 4.1 Combustion Front Velocity Versus Propagation Distance in Three Hydrogen-Air Mixtures at 300K and 0.1 MPa

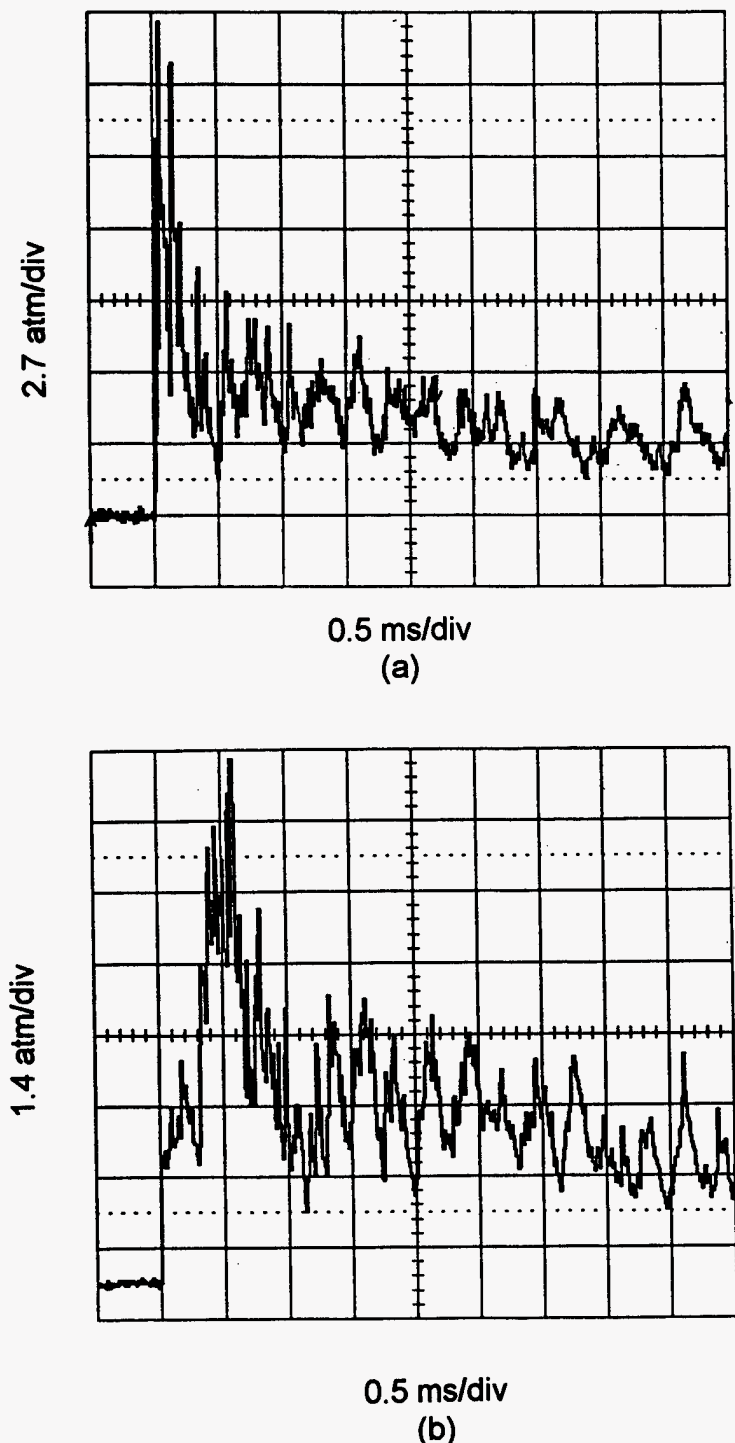


Figure 4.2 Typical Pressure Time History Corresponding to a;
(a) Detonation Wave, (b) Deflagration in the Choking Regime

4. Experimental Results

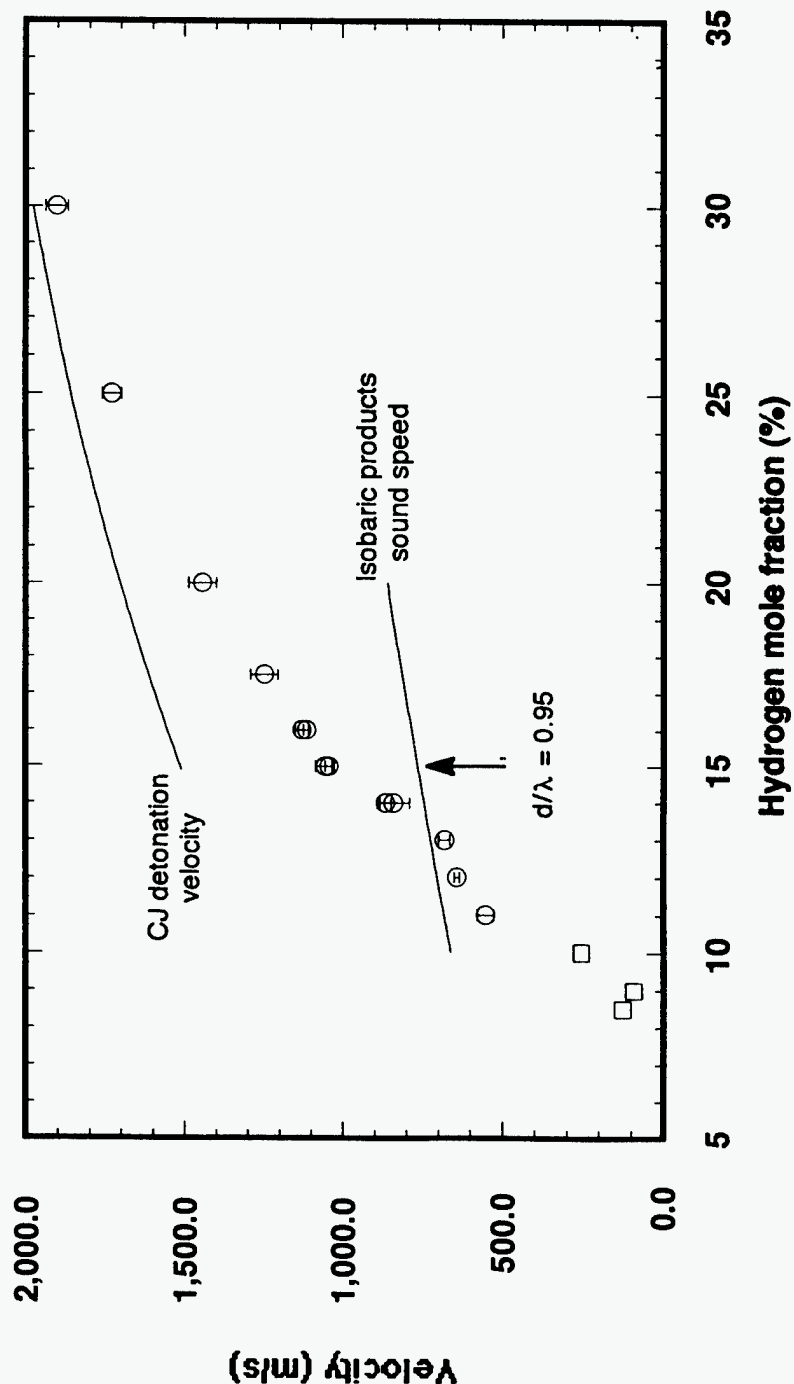


Figure 4.3 Combustion Front Velocity Versus Hydrogen Mole Fraction for Hydrogen-Air Mixtures at 300K and 0.1 MPa. Open circles denote the average velocity over roughly the second half of the vessel and error bars represent the standard deviation in the measured velocities. Open squares denote the maximum flame velocity for slow deflagrations

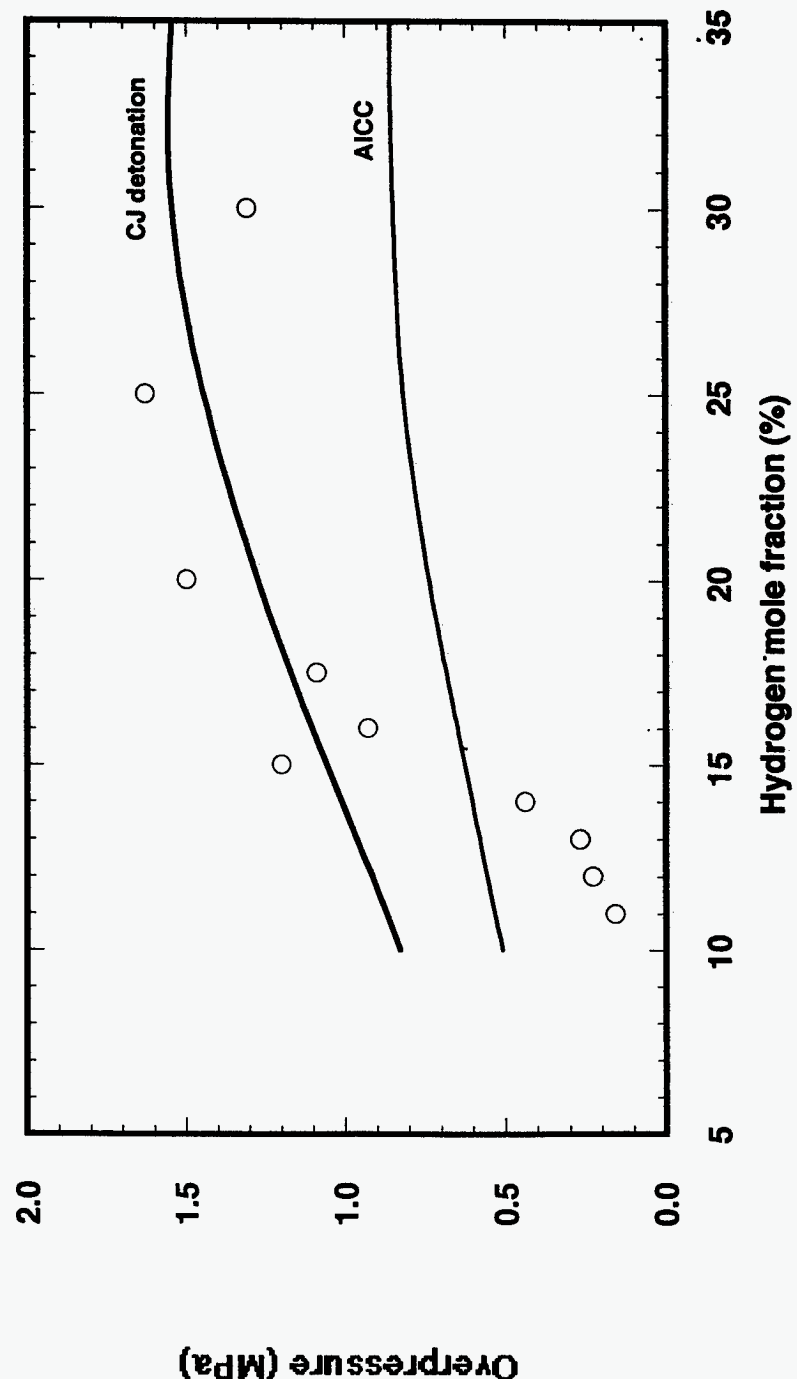


Figure 4.4 Comparison of the Measured Peak Overpressure for Hydrogen-Air Mixtures at 300K and 0.1 MPa and the Theoretical AIICC and CJ Detonation Pressure

4. Experimental Results

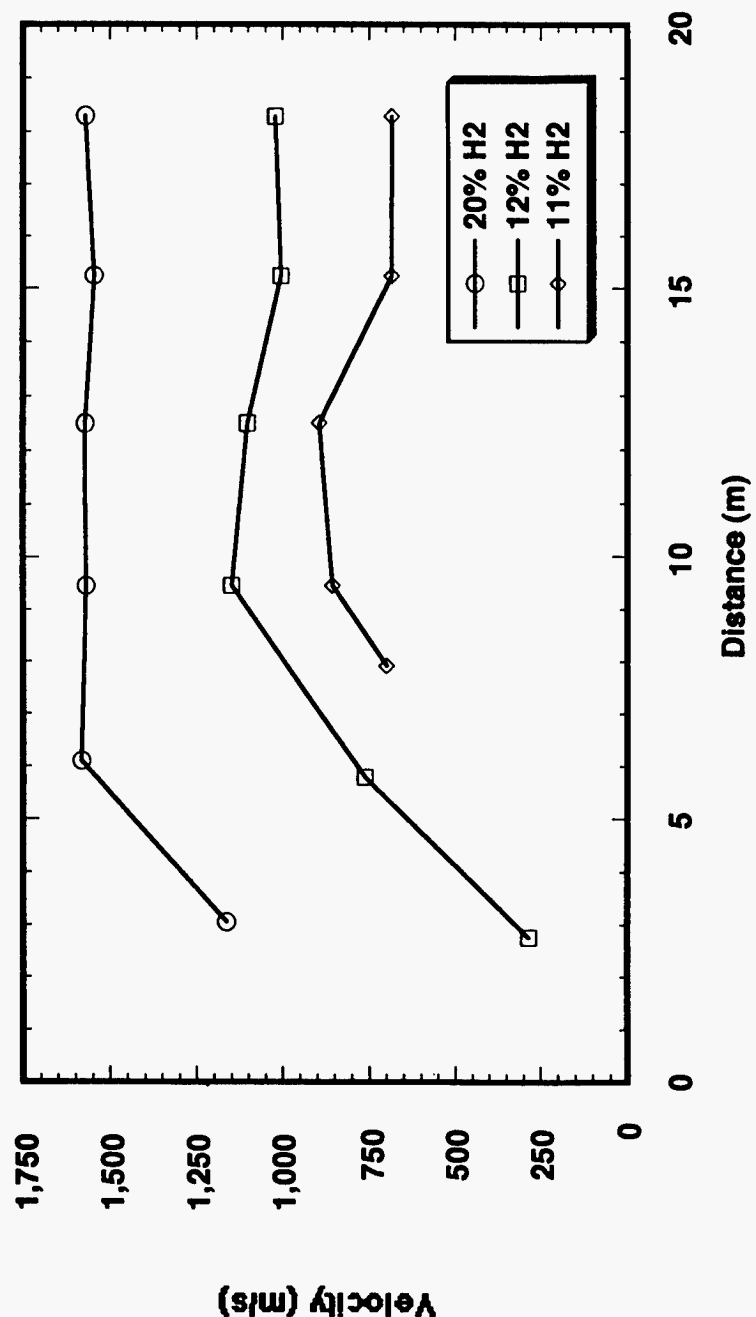
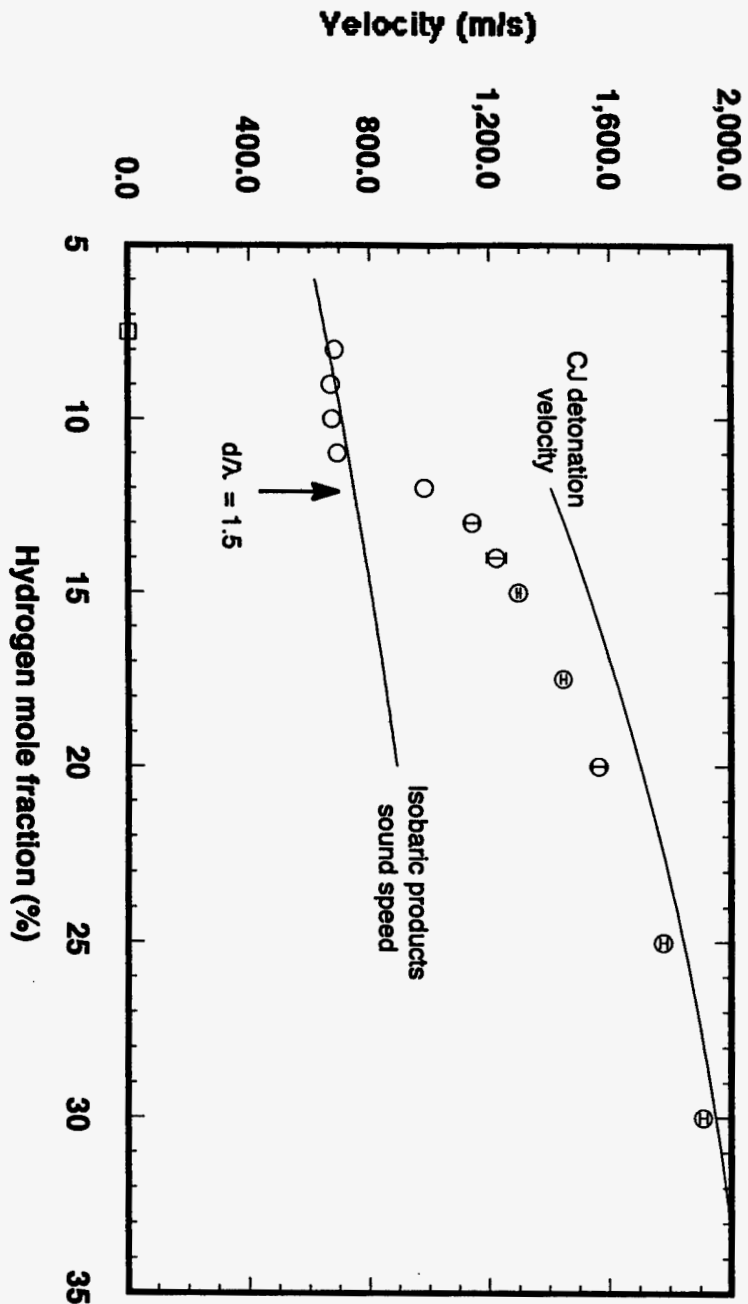


Figure 4.5 Combustion Front Velocity Versus Propagation Distance in Three Hydrogen-Air Mixtures at 500K and 0.1 MPa

Hydrogen-Air Mixtures at 500K and 0.1 MPa. Open circles denote the average velocity over roughly the second half of the vessel and error bars represent the standard deviation in the measured velocities. Open squares denote the maximum flame velocity for slow deflagrations

Figure 4.6



4. Experimental Results

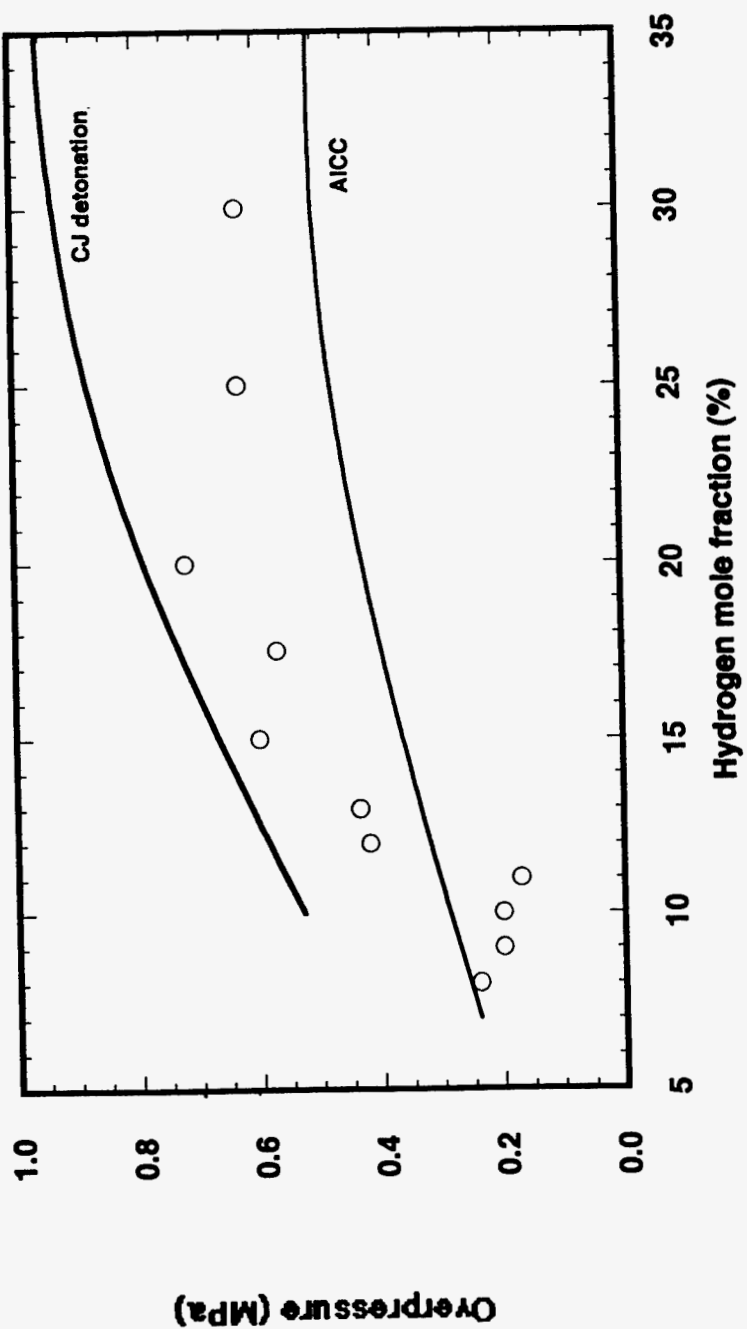


Figure 4.7 Comparison of the Measured Peak Overpressure for Hydrogen-Air Mixtures at 500K and 0.1 MPa and the Theoretical AICC and CJ Detonation Pressure

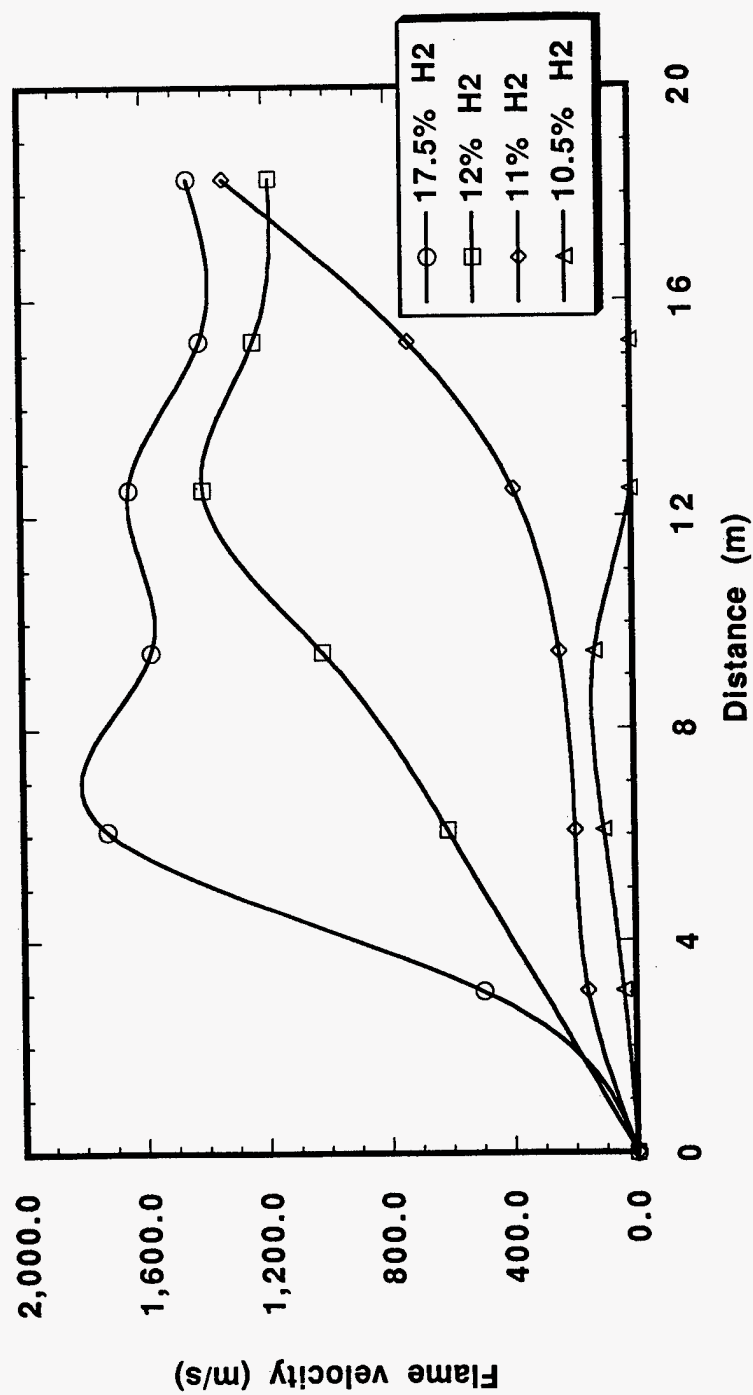


Figure 4.8 Combustion Front Velocity Versus Propagation Distance in Four Hydrogen-Air Mixtures at 650K and 0.1 MPa

4. Experimental Results

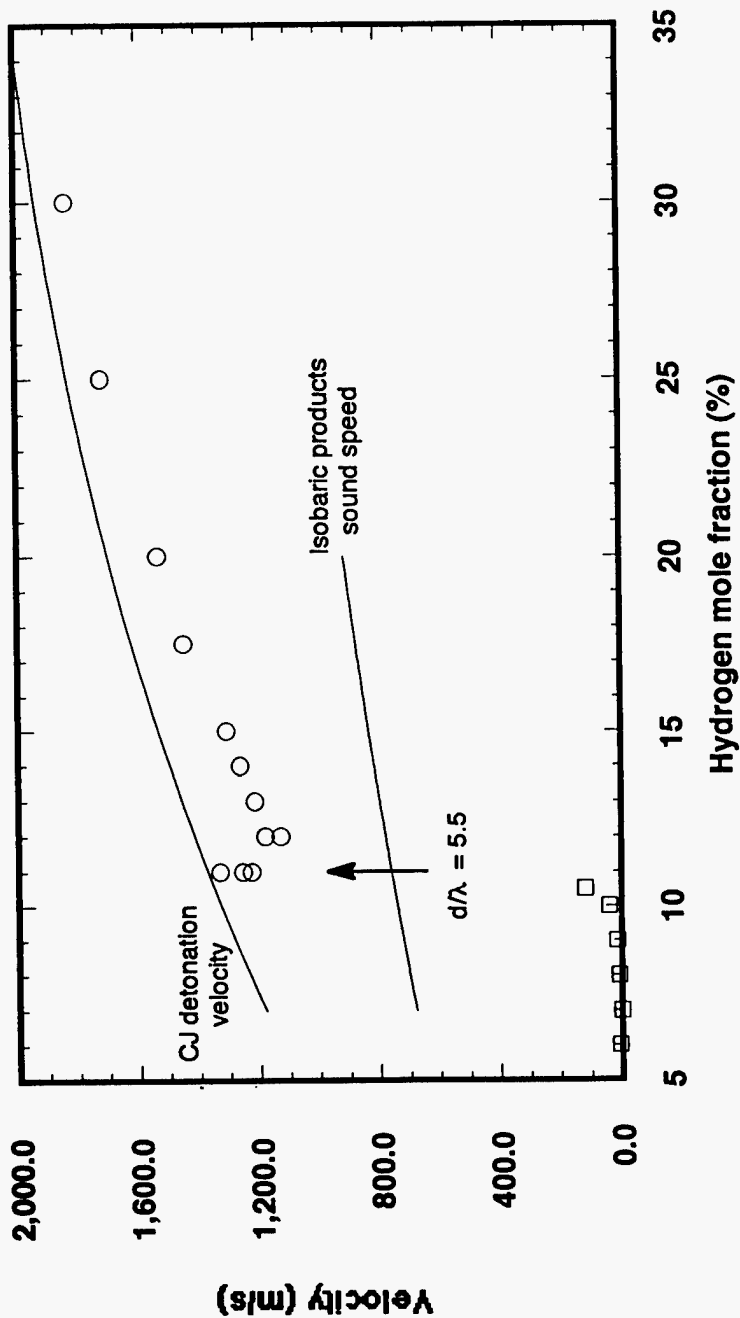


Figure 4.9 Combustion Front Velocity Versus Hydrogen Mole Fraction for Hydrogen-Air Mixtures at 650K and 0.1 MPa. Open circles denote the final velocity measurement in the vessel. Open squares denote the maximum flame velocity for slow deflagrations.

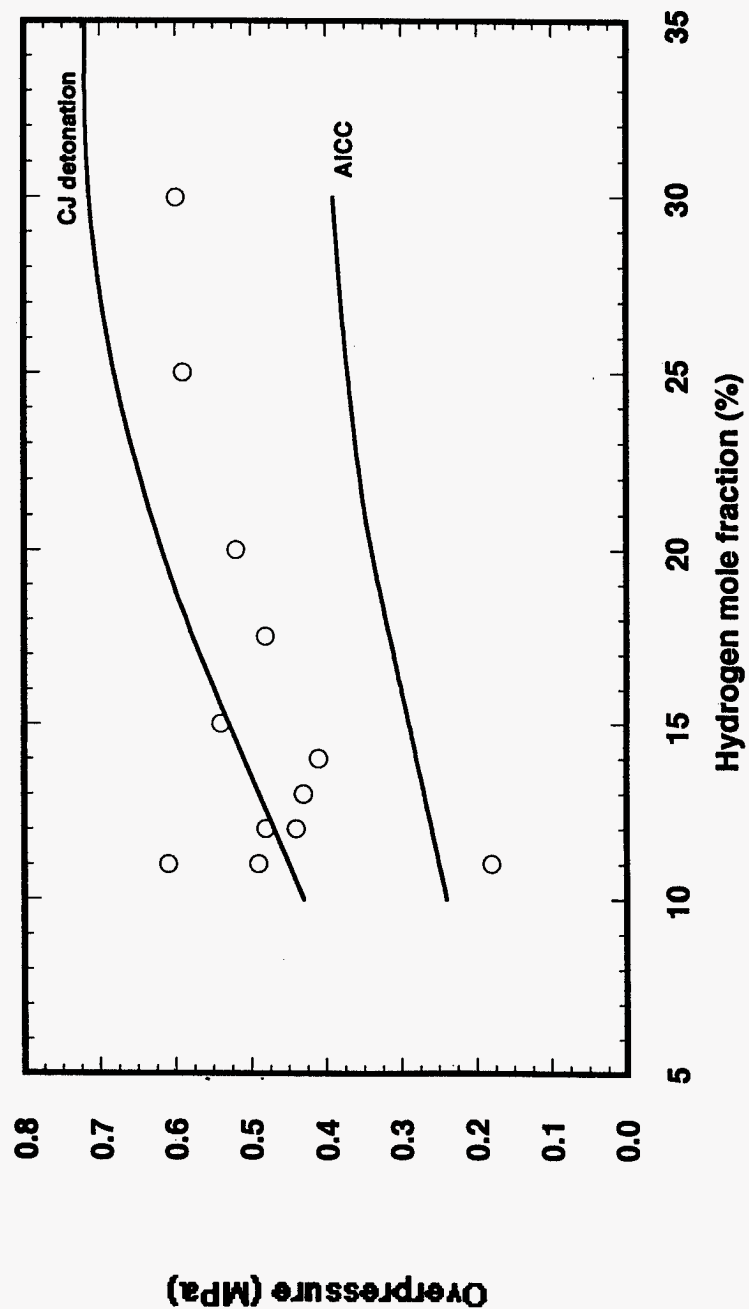


Figure 4.10 Comparison of the Measured Peak Overpressure for Hydrogen-Air Mixtures at 650K and 0.1 MPa and the Theoretical AICC and CJ Detonation Pressure

4. Experimental Results

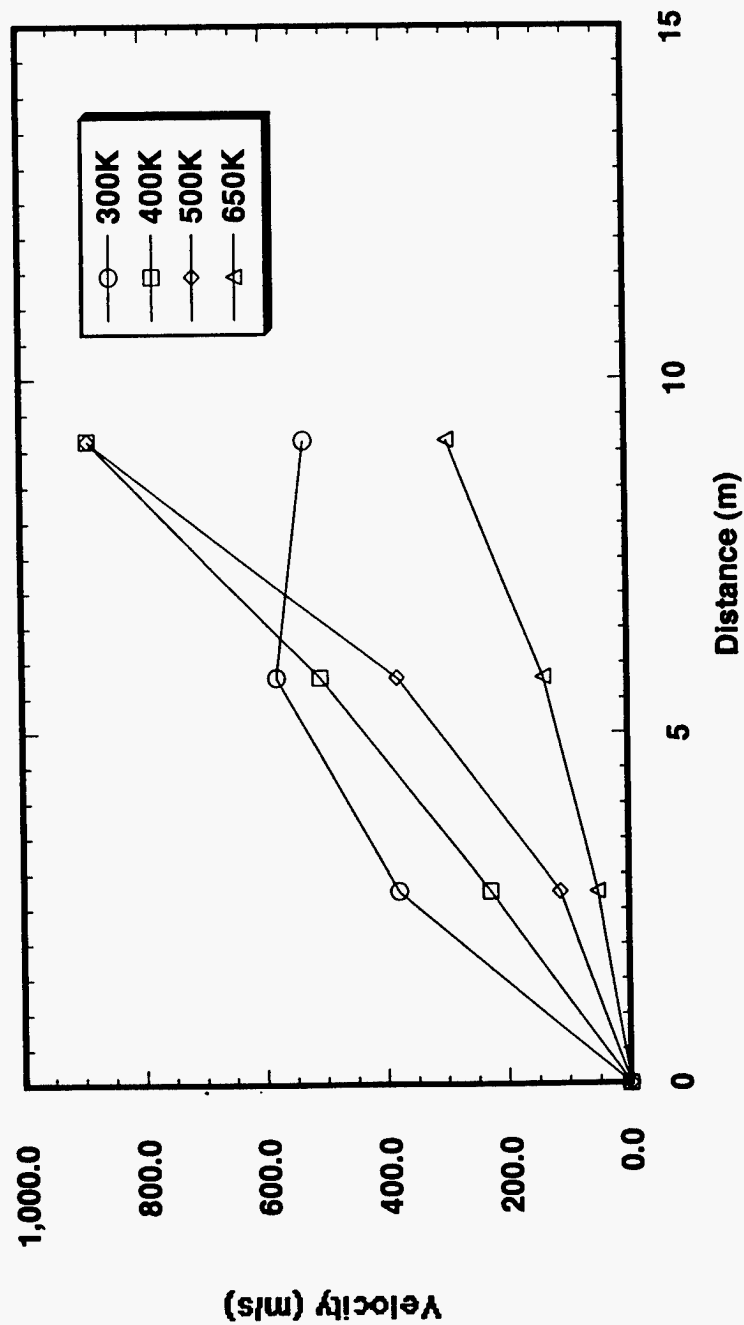


Figure 4.11 Combustion Front Velocity for a 11 Percent Hydrogen in Air Mixture at Four Different Initial Temperatures

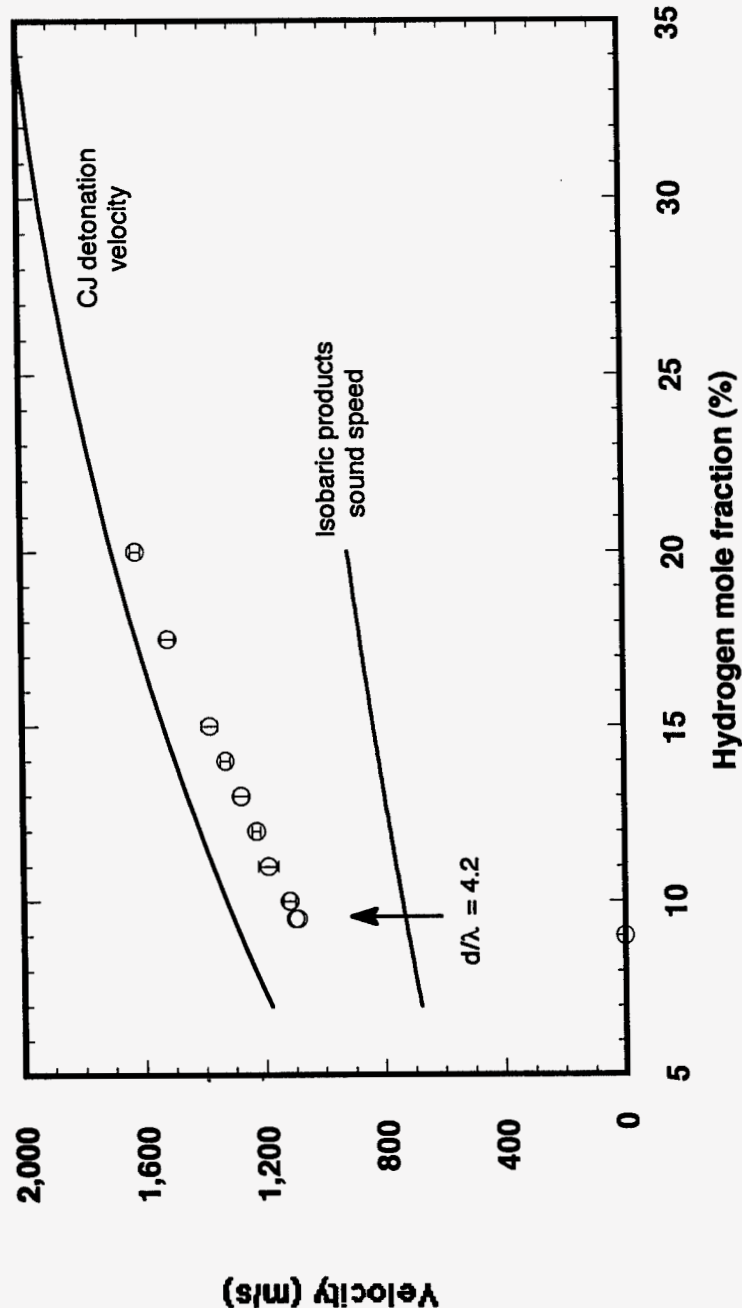


Figure 4.12 Combustion Front Velocity Versus Hydrogen Mole Fraction for Hydrogen-Air Mixtures at 650K and 0.1 MPa with the First Six Meters of the Vessel Maintained at 400K. Open circles denote the average velocity over roughly the second half of the vessel and error bars represent the standard deviation in the measured velocities.

4. Experimental Results

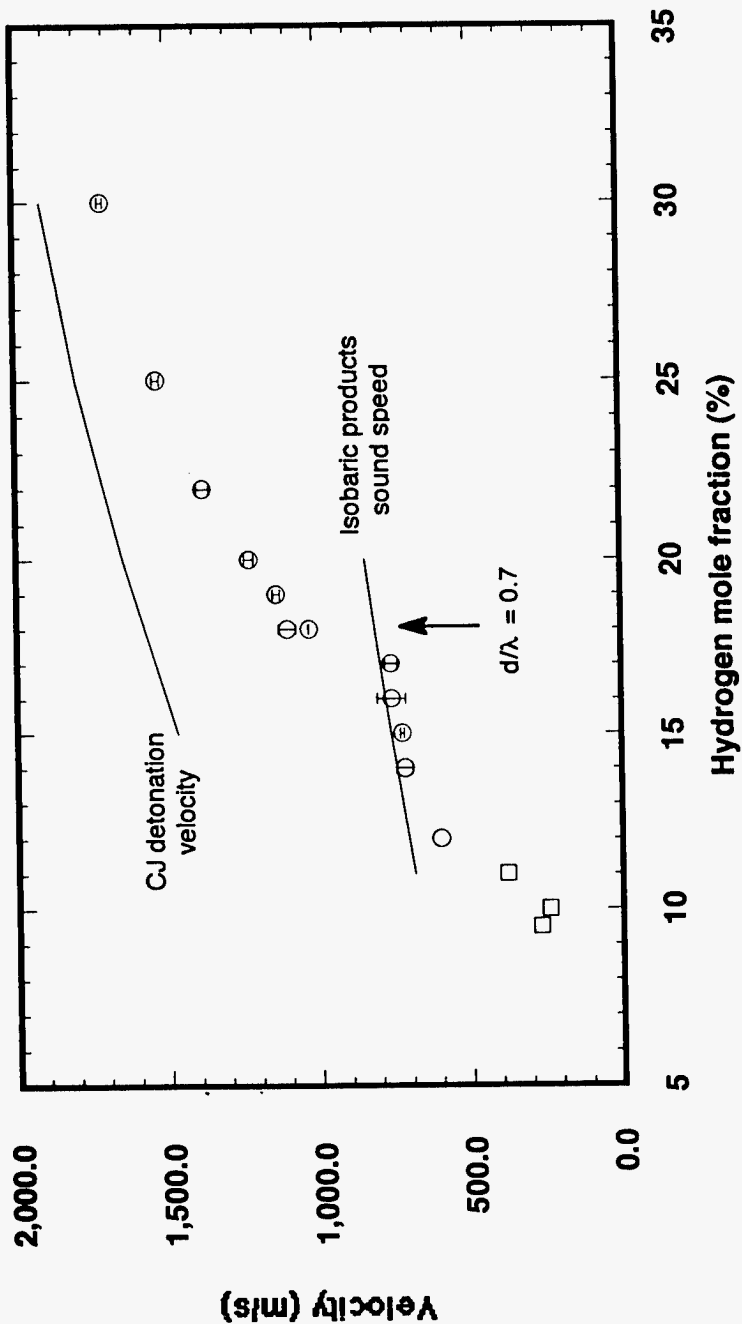


Figure 4.13 Combustion Front Velocity Versus Hydrogen Mole Fraction for Hydrogen-Air Mixtures with 10 Percent Steam at 400K and 0.1 MPa. Open circles denote the average velocity over roughly the second half of the vessel and error bars represent the standard deviation in the measured velocities. Open squares denote the maximum flame velocity for slow deflagrations

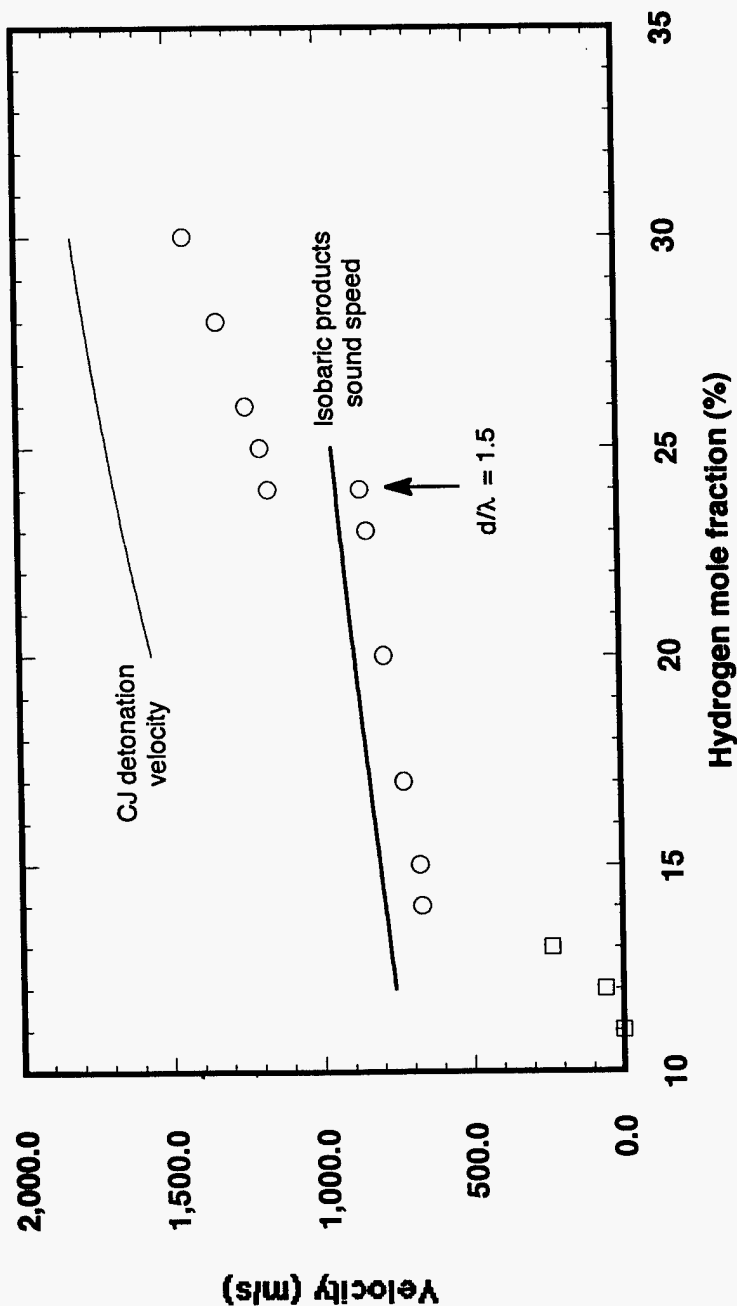


Figure 4.14 Combustion Front Velocity Versus Hydrogen Mole Fraction for Hydrogen-Air Mixtures with 25 Percent Steam at 500K and 0.1 MPa
 Open circles denote the average velocity over roughly the second half of the vessel and error bars represent the standard deviation in the measured velocities. Open squares denote the maximum flame velocity for slow deflagrations

4. Experimental Results

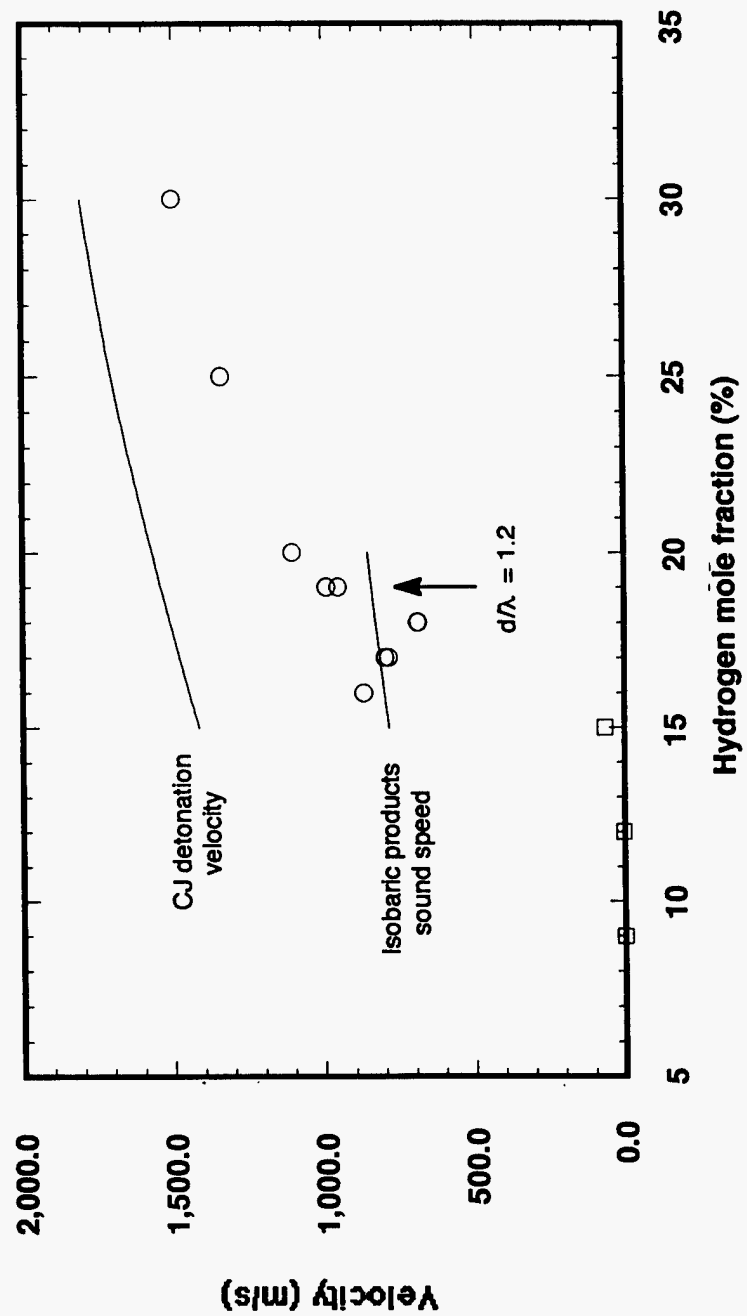


Figure 4.15 Combustion Front Velocity Versus Hydrogen Mole Fraction for Hydrogen-Air Mixtures with 25 Percent Steam at 650K and 0.1 MPa
Open circles denote the final velocity measurement in the vessel.
Open squares denote the maximum flame velocity for slow deflagrations

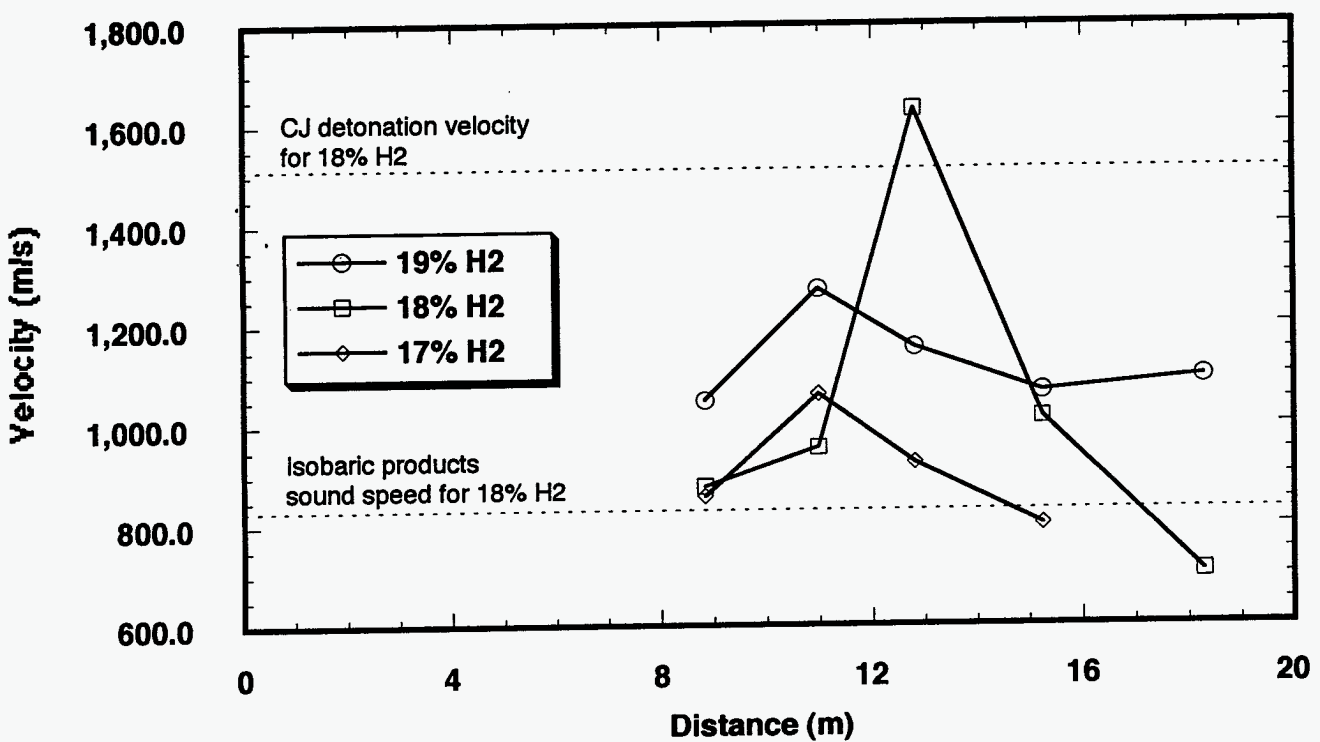
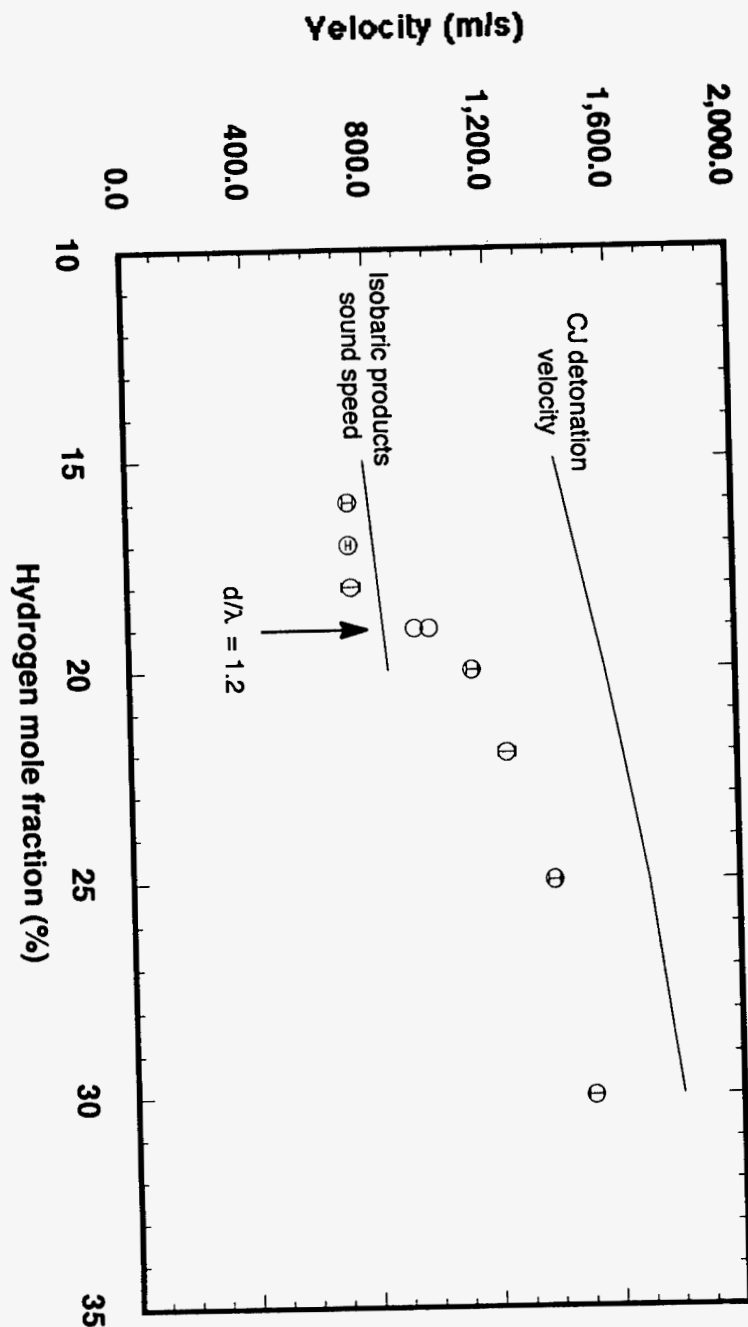


Figure 4.16 Combustion Front Velocity Versus Propagation Distance in Three Hydrogen-Air Mixtures with 25 Percent Steam at 650K and 0.1 MPa

velocities. Open squares denote the maximum flame velocity for slow deflagrations of the vessel and error bars represent the standard deviation in the measured Open circles denote the average velocity over roughly the second half the First Six Meters of the Vessel Maintained at 400K Hydrogen-Air Mixtures with 25 Percent Steam at 650K and 0.1 MPa with Combustion Front Velocity Versus Hydrogen Mole Fraction for the First Six Meters of the Vessel Maintained at 400K

Figure 4.17



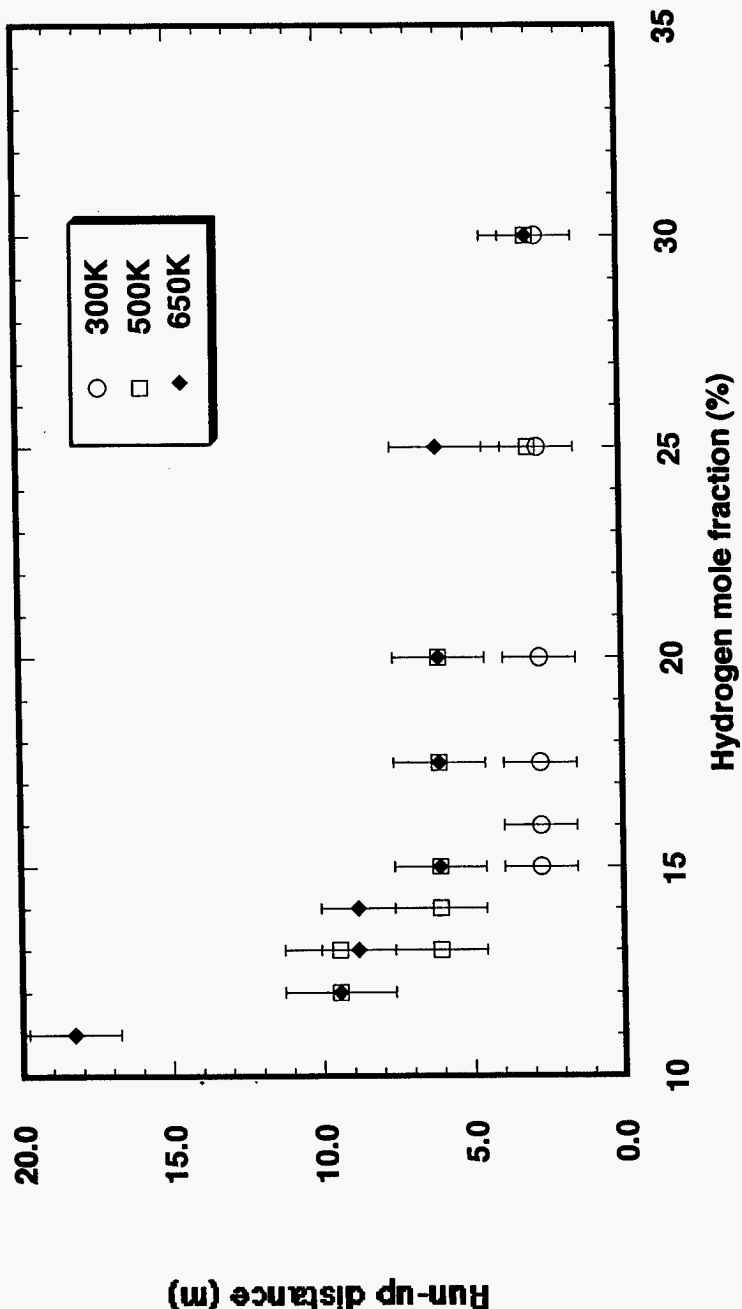


Figure 4.18 Measured Detonation Run-Up Distance for Hydrogen-Air Mixtures at Three Initial Temperatures

5. DISCUSSION

A key question that must be answered when predicting pressure loads in a nuclear reactor containment building resulting from a hydrogen burn is whether or not a detonation can be initiated as a result of flame acceleration. Knowledge of the applicability of the DDT limit criterion (i.e., d/λ) for the expected hydrogen-air-steam mixtures and a qualitative sense of the effect of initial mixture conditions such as temperature on the DDT run up distance are crucial for the analysis. The DDT limit criterion provides a scaling law which can be used to predict for a given compartment the minimum hydrogen concentration required for DDT. The DDT criterion is useful because no knowledge of the complexities of the flame acceleration process is needed; the only input needed is the detonation cell size of the mixture. The DDT run-up distance also provides a criterion on the length of the compartments under which a detonation may be initiated as a result of an accelerating flame. The containment pressure resulting from combustion, prior to DDT, is governed by the run-up distance. The containment pressure prior to DDT is an important parameter since the final detonation pressure loading on the containment is linearly proportional to this pre-DDT containment pressure. The run-up distance is intimately coupled to the details of the flame acceleration process, largely governed by the boundary conditions. Therefore, the run-up distances measured in the present experiments are unique to the apparatus and cannot be scaled. However, the observed effect of parameters, such as hydrogen mole fraction and initial temperature, can be used qualitatively in analyzing the potential for DDT in a given geometry.

5.1 Flame Acceleration

One of the main observations from the present experiments is that the rate of flame acceleration decreases with decreasing hydrogen mole fraction and decreases with increasing initial temperature. Similar observations were made by Beauvais et al. (1993) in their tests using orifice plates with a blockage ratio of 0.32. This effect manifests itself in the experimentally measured DDT run-up distance. For example, the run-up distance is observed to increase with decreasing hydrogen mole fraction and increasing initial temperature.

5.1.1 Flame Acceleration Mechanism

In this section, we will determine what are the important parameters which govern the process of flame acceleration and what the effect of increased temperature has on these parameters. Let us consider a flame initiated at the closed end of a tube, as shown schematically in Figure 5.1. For the analysis, a control volume encompassing the burnt gas, bounded by the tube wall and the convoluted flame sheet, is considered. In the analysis, we are assuming the velocity of the product gases is zero. This assumption will not be appropriate at higher flame velocities due to the presence of expansion and compression waves reverberating within the burnt gas. Applying the principle of conservation of mass to the control volume and assuming that the density of the unburnt gas ahead of the flame is uniform, one gets the time rate of change of the mass of the burnt gas to be

$$dm/dt = \rho_u \int s dA \quad (1)$$

where m is the mass of the gas in the control volume (i.e., the burnt gas), t is time, s is the local burning velocity, dA is a unit area of the flame sheet, ρ is density, and subscripts b and u correspond to the burnt and unburnt gas, respectively. In using Equation (1), we are assuming, as mentioned above, that combustion

5. Discussion

takes place over a continuous reaction sheet which is wrinkled by the turbulence. In this combustion regime, the combustion is rapid compared to the turbulent processes, or the flame thickness is small compared to the smallest turbulence length scale (commonly referred to as the Kolmogorov scale).

If we assume uniform density within the control volume, which is consistent with the assumption of uniform density within the unburnt gas, we can expand the left-hand term in Equation (1)

$$\rho_b A_{cs} V_f = \rho_u \int s dA \quad (2)$$

where A_{cs} is the tube cross-sectional area and V_f is the global flame velocity which from Equation (2) can be solved to be

$$V_f = (\rho_u / \rho_b) 1 / A_{cs} \int s dA \quad (3)$$

Without loss of generality, we can consider the burning velocity to be constant over the entire flame surface (in reality this is not true because of local curvature and flame stretch effects), yielding

$$V_f = (\rho_u / \rho_b) (s) (A_f / A_{cs}) \quad (4)$$

From Equation (4), we see that the flame velocity is a function of three parameters: (1) the density ratio across the flame, (2) the local burning velocity, and (3) the ratio of the flame surface area, A_f , and the tube cross sectional area. If we assume that the vessel pressure remains fairly constant over time, such that the density ratio term is constant, flame acceleration (i.e., dV_f/dt) is governed by the time rate of change of the burning velocity and flame area.

A flame generally follows the velocity flow field in the unburnt gas ahead of the flame. For low flame velocities in a smooth tube, the flow ahead of the flame is laminar, and the flame takes on a parabolic shape. In an obstacle-laden tube, such as the one used in the present experiments, the velocity flow field ahead of the flame is dictated by the boundary conditions. In a tube filled with orifice plates, one would expect a flow field shown in Figure 5.2. The flame is severely folded as a result of the velocity distribution in the main flow generated by the flow restriction through the orifice plate. One of the outstanding features in Figure 5.2 is that a standing eddy is formed downstream of each of the obstacles and is separated from the main flow by a shear layer. The total flame surface is comprised of the leading flame front as well as the flame surface associated with the burning of the unburnt gas eddies which are trapped behind each orifice plate. If the burnout time for these eddies is long compared to the average propagation time (e.g., tube length divided by the average flame velocity) of the flame front, one can see that the total flame surface area will increase in time resulting in flame acceleration. As the flame accelerates, larger gradients in the mean flow develop ahead of the flow leading to increased flame front surface area due to flame folding. The increase in the flame front surface area will be limited by flame stretching. The amount of flame area increase associated with the trapped pockets can exceed any flame area enhancement at the flame front due to flame folding. If the eddy burnout time is short compared to the average flame front propagation time, then the contribution of the flame area in the pockets is negligible.

5. Discussion

Experimentally, it was observed that for lean mixtures, the flame accelerates over a short distance and then decelerates. It is possible that the initial acceleration is due to the area increase associated with the point ignition. Once the flame is fully developed across the tube, since the flame velocity is fairly slow, the pockets burn out on the same time scale that the flame is propagating between orifice plates. Therefore, the pockets do not contribute to flame area and thus flame acceleration ceases. A second effect is that for very slow flames the burnt gas cools at the end of the tube so the gas contracts. This contraction sends out expansion waves which reach the flame and retard its progress.

If the induced gas flow ahead of the flame is laminar, the local burning velocity equals the laminar burning velocity for the mixture. The laminar burning velocity can be considered to be a fundamental property of the mixture which depends on the diffusivity and characteristic chemical reaction time of the mixture. If the flow ahead of the flame is turbulent, the burning velocity will be higher than the laminar burning velocity and will depend on the turbulence intensity which is typically measured in terms of the turbulent kinetic energy in the mean flow. The turbulent burning velocity is higher than the laminar burning velocity because of the enhanced transport properties associated with turbulence. The Reynolds number, defined as the ratio of the inertia forces and the viscous forces, is used as a criterion for laminar and turbulent flow. The Reynolds number is given by

$$Re = Ud/v \quad (5)$$

where U is the mean flow velocity, d is the pipe diameter, and v is the kinematic viscosity of the gas.

The relationship between the mean flow velocity ahead of the flame and the flame velocity can be determined by applying conservation of mass across the flame. By fixing the control volume to the flame, as shown in Figure 5.3, conservation of mass yields

$$\rho_b V_f = \rho_a s = \rho_a (V_f - U) \quad (6)$$

and with further manipulation,

$$U = [(\rho_a/\rho_b - 1)/(\rho_a/\rho_b)] V_f \quad (7)$$

Therefore, the Reynolds number of the flow ahead of a flame propagating at a steady velocity can be calculated using Equations (5) and (7). It is generally accepted that in commercial pipes, the transition from laminar to turbulent flow occurs at a Reynolds number of 2300. In general, the critical Reynolds number lies in the range of 2000 and 4000 depending on the wall roughness (Holman, 1981). If we take 2000 to be the critical Reynolds number, due to the large effective roughness associated with the orifice plates, we can calculate the critical flame velocity for a given mixture and initial temperature which results in turbulent flow ahead of the flame. If we consider a 10 percent hydrogen mixture, the density ratio and the kinematic viscosity at 300K are 3.48 (based on STANJAN calculation) and $25.1 \times 10^{-6} \text{ m}^2/\text{s}$ (Holman, 1981), respectively. At 650K, the density ratio and the kinematic viscosity are 2.1 and $92.9 \text{ m}^2/\text{s}$. Based on a critical Reynolds number of 2000, the critical flame velocity at 300K is 0.3 m/s, and at 650K, it is 2.0 m/s. Using Equation (6), these flame velocities correspond to burning velocities of 0.1 m/s and 1.0 m/s for 300K and 650K, respectively. These critical burning velocities are both below the laminar burning velocities for 10 percent hydrogen at the

5. Discussion

respective temperatures. For example, for a 10 percent hydrogen mixture at 300K and 650K, the laminar burning velocity is 0.4 m/s and 1.5 m/s, respectively (Liu and MacFarlane, 1983). Therefore, the flow ahead of the flame is turbulent for all steady flame velocities.

According to Equation (7), as the flame accelerates, the flow velocity ahead of the flame increases and thus the turbulence intensity increases. The increased turbulence intensity enhances the transport properties and thus the local turbulent burning velocity increases. Several correlations relating the turbulent burning velocity with the laminar burning velocity, the mean flow velocity, and the turbulence intensity have been proposed in the past (Lefebvre and Reid, 1966). For our purpose, we can assume that the turbulence intensity is proportional to the mean flow velocity and thus the following simple relationship can be considered

$$S_T/S_L \propto U \quad (8)$$

From the above analysis, we can better see the feedback mechanism which is essential for flame acceleration. An increase in the flame velocity causes an increase in the flow velocity ahead of the flame through Equation (7). The increased flow velocity causes both an increase in the turbulent burning velocity through Equation (8) and increased flame surface area as a result of increased flame folding. In turn, both the increased flame folding and burning velocity yield further flame acceleration via Equation (4).

5.1.2 Influence of Initial Temperature on Flame Acceleration Parameters

From Equations (4) and (7), we can see that one of the most important parameters which governs the flame acceleration process is the the ratio of the unburnt to the burnt gas density (ρ_u/ρ_b). This parameters dictates how much the gas expands after crossing the flame and as a result determines how much flow is generated ahead of the flame. In the present study, the following observations have been made concerning the rate of flame acceleration: (1) for a fixed hydrogen mole fraction, the flame acceleration rate decreases with increasing initial temperature (see Figure 4.11), (2) for a fixed temperature, the flame acceleration rate decreases with decreasing hydrogen mole fraction, and (3) for a given hydrogen mole fraction and initial temperature, the flame acceleration rate decreases with increases steam dilution. All three of these effects resulting in a decreased flame acceleration rate are consistent with a decrease in the magnitude of (ρ_u/ρ_b), as demonstrated in Table 5.1 below.

5. Discussion

Table 5.1 Density Ratio Across the Flame and the Laminar Burning Velocity as a Function of Temperature and Mixture Composition

Temperature (K)	Hydrogen (%)	Steam Dilution (%)	(ρ_u/ρ_b)	Burning Velocity (m/s)
300	11	0	3.7	0.5
500			2.6	1.2
650			2.2	1.9
300	30	0	6.9	2.5
	20		5.5	1.4
	10		3.5	0.4
500	10	0	2.4	1.0
			2.0	0.6

The values for (ρ_u/ρ_b) in the above table were calculated using the chemical equilibrium code STANJAN (Reynolds, 1986) for a constant pressure burn. Also given in Table 5.1 are the corresponding laminar burning velocity from Liu and MacFarlane (1983). The laminar burning velocity is a fundamental parameter which also influences flame acceleration since it influences the turbulent burning velocity. Just as increasing the density ratio across the flame increases the rate of flame acceleration, so does increasing the laminar burning velocity. From Table 5.1, we see that, except for increasing temperature, there is a similar trend between the density ratio and the laminar burning velocity. Increasing the temperature increases the laminar burning velocity and decreases the density ratio, which result in opposing effects on flame acceleration. From the experimental data, it is clear that the rate of flame acceleration decreases with increasing initial temperature, and thus, based on this simple model the density ratio effect dominates.

The most serious assumption made in the above analysis concerns the simple relationship used to calculate the turbulent burning velocity (see Equation (8)). Since the laminar burning velocity is a constant, it is assumed that the turbulent burning velocity is a function of only the mixture flow velocity ahead of the flame. Empirical turbulent burning velocity correlations have proposed which include the turbulent Reynolds number as a parameter (Bradley et al., 1992). For a given length scale and velocity the Reynolds number is inversely proportional to the kinematic viscosity, see Equation (5). For air the kinematic velocity increases by a factor of 2 between 300K and 650K, and thus the Reynolds number decreases by a factor of two. Therefore, if one assumes that the turbulent burning velocity is a function of the Reynolds number this could be another factor which could be used to explain the observed reduced flame acceleration at 650K.

The DDT run-up distance is defined as the distance required for the flame to accelerate to the point of DDT. Based on this definition, it is clear that the DDT run-up distance depends on the flame acceleration rate which is dependent on the turbulence generated by the obstacles in the tube. Another parameter which influences the run-up distance is the sound speed in the unburnt gas ahead of the flame. As the flame accelerates, it continuously generates compression waves ahead of it; when these waves coalesce, a shock wave is formed. With continuing flame acceleration, the shock increases in strength as more and more compression waves

5. Discussion

merge with the leading shock wave. Eventually, this shock wave strengthens to the point where a detonation is initiated behind the shock wave and overtakes it. For a given flame velocity time history, the distance from the ignition point where a shock is formed depends on the speed of sound of the gas (Thompson, 1972). For a given flame velocity-time history, the higher the speed of sound, the longer the distance required for shock wave formation. The sound speed, c , in an ideal gas is given by

$$C^2 = \gamma R T \quad (9)$$

where γ is the ratio of the specific heats, R is the universal gas constant divided by the molecular weight of the gas, and T is temperature. The above expression indicates that the speed of sound is proportional to the square root of the gas temperature and inversely proportional to the molecular weight. Since hydrogen is a very light compared to air, it has a fairly high speed of sound relative to air. Therefore, the hydrogen mole fraction, as well as the steam mole fraction, influences the speed of sound of the mixture. The following table demonstrates the relative influence of gas temperature, hydrogen mole fraction, and steam dilution on the speed of sound in the mixture.

Table 5.2 Speed of Sound in the Unburnt Mixture

Temperature (K)	Hydrogen (%)	Steam Dilution (%)	C (m/s)
300	10	0	364
500			469
650			532
300	30	0	409
	20		385
	10		364
500	10	0	469
		25	485

The speed of sound in the above table was calculated using STANJAN (Reynolds, 1986). From the above table, one can see that the gas temperature has the most dominant effect on the speed of sound of the mixture. Steam has very little influence since its molecular weight isn't that different from air. Even though, there is a large difference between the molecular weight of hydrogen and air, there is little effect on sound speed since hydrogen is typically the smaller component of the two. So the mixture initial temperature has the greatest effect on the speed of sound and thus the greatest effect on the distance required to form a shock wave via an accelerating flame.

In summary, the DDT run-up distance depends both on the rate of flame acceleration and distance required for a shock wave to form. Increasing the mixture initial temperature decreases (ρ_a/ρ_b) which decreases the flame acceleration rate. Increasing the mixture initial temperature also increases the speed of sound which increases the distance required for the shock wave to be formed. Therefore, increasing the mixture initial temperature adversely effects both these parameters and as a result increases the DDT run-up distance.

5. Discussion

5.2 DDT Limit Criterion

Experiments carried out at McGill University (Guirao et al., 1989) in an obstacle-laden tube, very similar to the one used in the present experiments, demonstrated that the limit for DDT could be correlated with the orifice inner diameter and the mixture detonation cell size. The experimental results indicated that DDT occurred in mixtures where $d/\lambda > 1$; that is, when the orifice opening could accommodate at least one detonation cell. From this, one can propose a general DDT limit criterion $d/\lambda = 1$, which fixes the minimum hydrogen composition mixture which can result in a DDT in a given geometry.

The McGill experimental results, obtained in mixtures at an initial temperature of 300K, have been reproduced in the present experiments. These experiments have shown that in general the $d/\lambda = 1$ DDT limit criterion applies at different initial temperatures, with and without steam. The only exception was in tests performed in dry hydrogen-air mixtures at an initial temperature of 650K. In these tests, DDT was observed in mixtures with greater than or equal to 11 percent hydrogen, which corresponds to a value of d/λ equal 5.5. Although this result does not violate the $d/\lambda > 1$ criterion for the possibility of DDT, it is at variance with the DDT limit of $d/\lambda = 1$ which was found to apply at all the other initial conditions.

In most cases, a plot of the final average flame velocity versus hydrogen mole fraction indicated that the DDT limit was a transitional limit between the choking and the detonation limit. For example, for a mixture slightly leaner in hydrogen, than the hydrogen mixture at the DDT limit, the flame was observed to accelerate to a constant velocity equal to the speed of sound in the products (i.e., choking regime). For flame propagation in the choking regime, the mixture between the precursor shock and the flame is in a compressed state. Therefore, the mixture behind the shock wave has been processed, and whether or not DDT will occur depends on many factors, such as physical length scales, mixture detonation cell size, gradients in temperature, vorticity, and many yet unknown parameters. The DDT limit is governed by the existence of a mixture state, consisting of a combination of these parameters, behind the precursor shock wave which is favorable to the initiation of detonation.

There is a fundamental difference in the observed DDT limit in dry hydrogen-air at 650K and that observed at all the other conditions. This difference is that in the dry hydrogen-air experiments at 650K, no flame propagation was observed in the choking regime. For the 10.5 percent hydrogen-air mixture, which is 0.5 percent leaner in hydrogen than the hydrogen-air mixture at the DDT limit, the flame velocity peaked at about 100 m/s at mid vessel and slowly decayed to the laminar burning velocity by the end of the tube. Therefore, the nonexistence of DDT at this condition can be attributed to the inability of the mixture to sustain flame acceleration to a point where the mixture ahead of the flame could be preconditioned by the precursor shock wave by either the generation of vorticity, temperature nonuniformities, or shock reflection. This is not to say that a shock wave is necessary to initiate a detonation. It is well known that a detonation can be initiated via a hot jet (Dorofeev, 1992) or by the nonuniform photo-dissociation of a gas (Lee et al., 1978). In both these cases, it has been argued that the detonation initiation is due to the SWACER mechanism resulting from the initial induction time gradient which exists in the mixture prior to initiation. In an obstacle-laden tube, flame acceleration is the process by which the above-mentioned gradients are produced which are required for the SWACER mechanism. Therefore, the observed DDT limit at 650K is an artifact of the inability of the flame to accelerate and not the inherent property of the detonability of the mixture.

5. Discussion

For hydrogen-air mixtures with 25 percent steam dilution at 650K, the DDT limit was found to be 19 percent hydrogen, which yields a value of $d/\lambda = 1.2$. This is in close agreement with the $d/\lambda = 1$ DDT limit criterion and corresponds to the transition from the choking regime to the detonation regime, as shown in Figure 4.14. Unlike the dry hydrogen-air mixtures at an initial temperature of 650K, the steam diluted mixtures leaner than the DDT limit were capable of accelerating to a velocity equal to the sound speed in the burnt products. As described in Section 5.1, the density ratio of the unburnt to the burnt gas and the mixture laminar burning velocity are key factors for determining flame acceleration. The density ratio across the flame and the laminar burning velocity for a 19 percent hydrogen in air mixture with 25 percent steam is 2.4 and 2.7 m/s, respectively. From Table 5.1, the density ratio and burning velocity in the dry 11 percent hydrogen in air mixture is 2.2 and 1.9 m/s, respectively. As described in Section 5.1, mixtures with a higher density ratios across the flame and burning velocity result in higher flame acceleration rates. This indicates that the potential for flame acceleration in the steam diluted DDT limit mixture (e.g., $d/\lambda = 1.2$) is higher than the dry 11 percent mixture which has a smaller cell size and thus a larger value of d/λ (e.g., 5.5).

It was also observed that DDT could be promoted by artificially increasing the flame acceleration rate. For example, in a 10 percent hydrogen mixture at 650K, flame acceleration was severely limited and no DDT was observed. DDT was observed in the same 10 percent hydrogen mixtures by promoting flame acceleration by keeping the first section of the vessel cold. Note, DDT occurred near the end of the tube, far removed from the colder gas in the first 6.1 meters of the tube. Therefore, the initial cold section acted only as a booster for the flame and had no direct role in the local DDT phenomenon. In the experiments carried out by Beauvais et al. (1993), enhancement of flame acceleration was achieved by using higher blockage ratio orifice plates (e.g., $BR=0.7$) in the first half of the obstacle section. This resulted in DDT in mixtures which otherwise were nondetonable using the 0.3 BR orifice plates.

It is clear from the above discussion that the $d/\lambda=1$ criterion is a necessary but not sufficient condition for DDT in an obstacle-laden tube. The $d/\lambda=1$ criterion is actually a propagation limit similar to the $D/\lambda=1$ detonation limit observed in smooth tubes (Guirao et al., 1989), where D is the tube inner diameter. For example, in the 18 percent hydrogen mixture with 25 percent steam dilution at 650K, a detonation was initiated in the tube but subsequently failed resulting in flame propagation in the choking regime. As a result of the final propagation velocity, this flame propagation is considered to be in the choking regime below the DDT limit, even though the initiation of a detonation was observed. Of course, this can be considered to be a phenomenon which would occur for mixtures very close to the DDT limit, but nevertheless, it points out the implications of such a rigid DDT limit criterion.

When using the DDT criterion in a safety analysis to obtain a lower detonability limit for a given compartment there is a certain amount of conservatism built in since one is assuming that conditions exist within the compartment such that a flame can accelerate to the point where DDT can occur. Aside from direct initiation, which can be ruled out due to the large initiation energy required, the only other source of detonation initiation in a compartment is via the transmission of a detonation from an adjacent compartment or as a result of mixing with hot combustion products issuing from an adjacent compartment. For both these scenarios the detonation initiation criterion requires at least 10 to 13 cells to pass through the opening linking the adjacent compartments (e.g., $d_c = 13\lambda$, where d_c is the characteristic opening dimension). Since the opening dimension is smaller than the compartment overall size, d , (i.e., $d/d_c = k$ where $k > 1$) then the criterion for detonation initiation within a compartment as a result of a hot jet or the transmission of a detonation is $d = 13k\lambda$ which

5. Discussion

implies $d > 13\lambda$. For a given a given compartment size d , the maximum mixture cell size required for detonation initiation using the DDT criterion is $\lambda = d$ minimum, whereas using the transmission criterion the maximum cell size is $\lambda = d/13k$. Therefore, the $d = \lambda$ DDT criterion is more conservative then the transmission criterion since the detonability limit for a given compartment corresponds to a leaner hydrogen mixture.

5.3 Influence of Detonation Stability

Experiments in the past have demonstrated that correlations describing detonation phenomenon, involving the detonation cell size and a physical length scale breakdown for certain combustible mixtures. Shepherd et al. (1988) and Desbordes et al. (1993) demonstrated that heavy diluting of an acetylene-oxygen mixture with a monatomic inert gas, such as argon or helium, resulted in the failure of the classical dynamic detonation parameters linking the critical tube and critical energy with the detonation cell size (Lee, 1984). These types of mixtures are said to produce more stable detonation waves. Detonation phenomena are inherently unstable and the cellular structure of a detonation is the physical manifestation of this instability. In the context of this discussion, a stable detonation is then one in which the mixture's chemical induction time, τ_i , is insensitive to postshock temperature fluctuations. The chemical induction time is dependent on the post shock temperature, T , via the Arrhenius factor $\tau_i \propto \exp(E/RT)$, where E and R are the global activation energy and the universal gas constant, respectively. We see that the lower the global activation energy or the higher the postshock temperature, the smaller the exponential and thus the less sensitive the induction time is to fluctuations in the post-shock temperature, or equivalently the shock mach number. The monatomic gas dilution cited above tends to increase the postshock temperature, thereby stabilizing the detonation. In general, stable detonations also display a very regular cellular structure (Ciccarelli et al., 1997).

The effect of increased initial temperature in a hydrogen-air mixture is to raise the post-shock temperature and lower the global activation energy (Ciccarelli et al., 1997). As described above, this tends to stabilize the detonation. If one extrapolates the argument that the correlations describing detonation phenomenon breakdown for stable detonations, one might expect that the $d/\lambda=1$ DDT limit correlation in obstacle-laden tubes fails at elevated temperatures. A breakdown in the DDT limit criterion has been observed for dry hydrogen-air mixtures at 650K. However, as discussed in Section 5.2, we attribute the variance in the experimentally observed DDT limit at 650K to the inability of the mixture to sustain flame acceleration. We do not attribute this breakdown in the criterion to detonation stability as characterized above. In essence, the flame never achieves a velocity where conditions are set up where detonation initiation can be considered; therefore, the observed DDT limit is governed by turbulent flame propagation mechanisms and not detonation properties, such as detonation stability. The evidence for this lies in the fact that the DDT limit could be influenced by changing the flame acceleration characteristics. It was shown that the observed DDT limit at 650K could be lowered by maintaining the first section of the vessel relatively cool. Maintaining the first section of the vessel cool resulted in a higher initial flame acceleration, however, the transition to detonation occurred within the heated section of the tube. Clearly for these experiments, the DDT limit observed is governed by the flame acceleration process and not by the local detonation initiation, which could be governed by the detonation stability arguments.

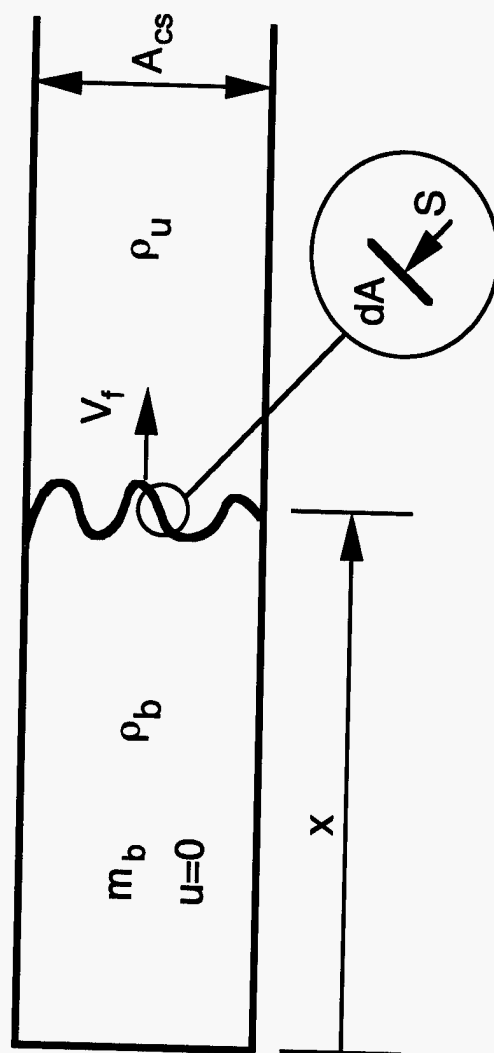


Figure 5.1 Schematic showing flame propagation in a closed-ended tube with appropriate nomenclature indicated

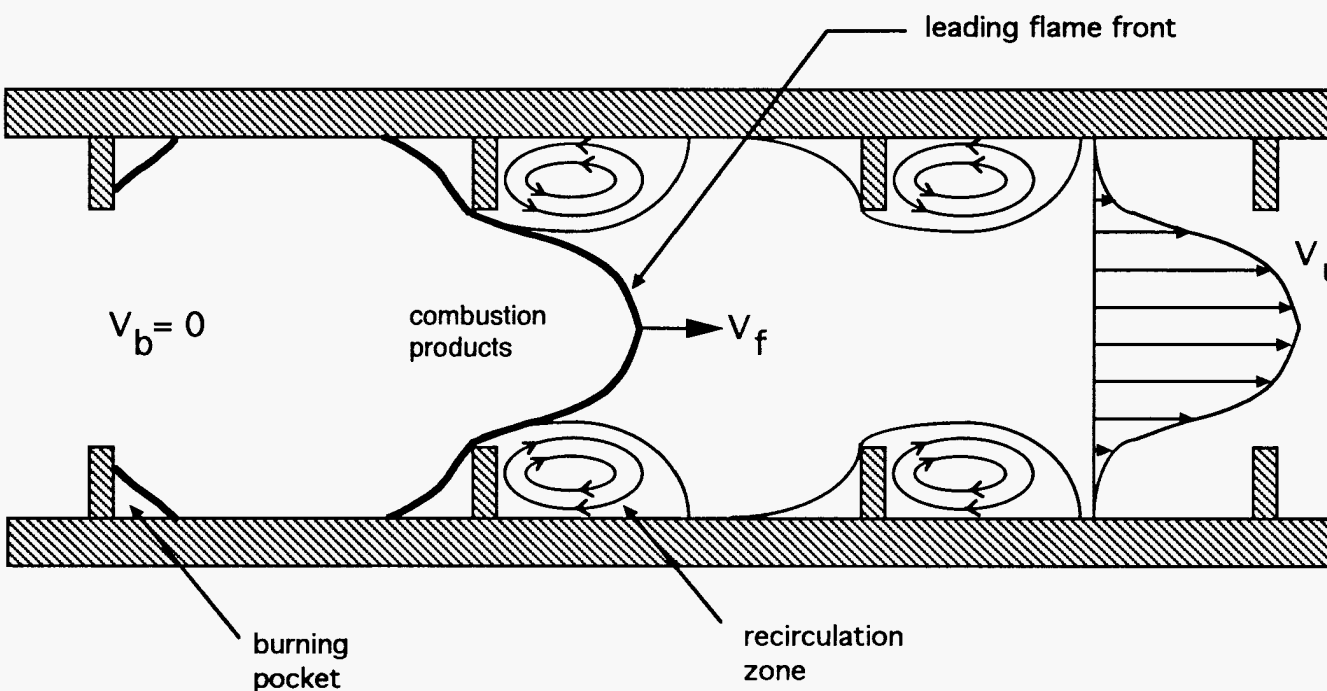


Figure 5.2 Schematic showing the velocity flow field generated ahead of a flame propagating in an obstacle-laden tube

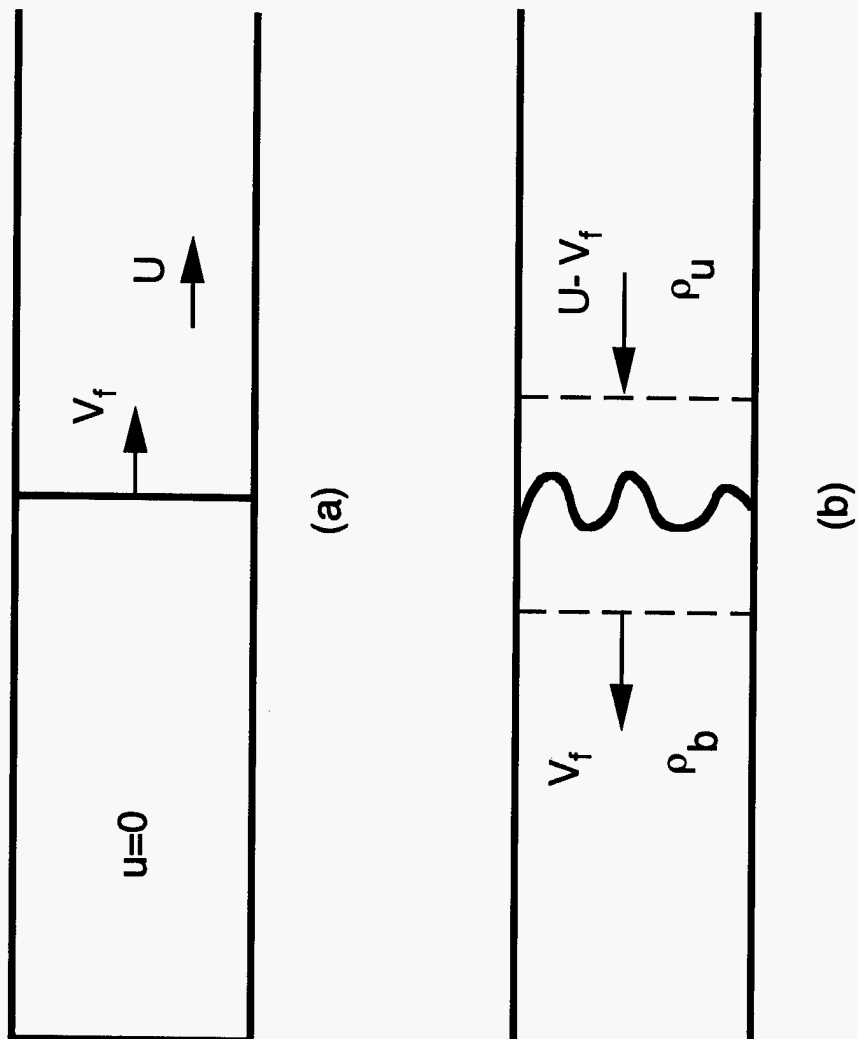


Figure 5.3 Schematic showing flame and unburnt flow velocity vectors in the (a) fixed reference frame and (b) reference frame moving with the flame

6. CONCLUSION

Results from an investigation into the influence of initial temperature on flame acceleration and DDT phenomenon in hydrogen-air-steam mixtures have been presented. Experiments were carried out in the HTCF equipped with orifice plates with a blockage ratio of 0.43. The limiting mixture composition and initial conditions for DDT are correlated with the detonation cell size.

Flame propagation in this geometry consists of an initial flame acceleration phase followed by a steady-state phase. The various flame propagation regimes observed have been classified and characterized as:

- (1) Detonation: Flame acceleration leads to the initiation of a detonation which propagates at a velocity typically just under the theoretical detonation velocity and a pressure just under the CJ detonation pressure.
- (2) Choking: The final steady-state flame velocity equals the speed of sound in the burnt gas and the pressure is typically just below the mixture AICC pressure.
- (3) Slow deflagrations: The final flame velocity is on the order of the laminar burning velocity. In these mixtures, the flame accelerates to a maximum velocity of 100-200 m/s and then decelerates to a velocity close to the laminar burning velocity.

In terms of potential vulnerability of nuclear power plant containment buildings to overpressures resulting from a hydrogen burn, the slow deflagration mode is the least severe (i.e., the containment pressure rises very slowly and there is no dynamic shock loading) and the detonation mode is most severe. However, flame propagation in the choking regime can also produce substantial pressure loads. In fact, the peak shock pressures from flame propagation in the choking regime, which are typically close to the AICC pressure, are comparable to the detonation pressure in lean hydrogen-air mixtures.

In the present experiments, for a given tube diameter and orifice size and spacing, DDT was observed in dry hydrogen-air mixtures at 300K, 500K, and 650K for hydrogen mole fractions in excess of 15, 12, and 11 percent, respectively. The choking limits at these temperatures were observed to be 11, 8, and 11 percent hydrogen, respectively. Note, at 650K, no flame propagation in the choking regime was observed. In hydrogen-air mixtures with 25 percent steam dilution at 500K and 650K, DDT was observed in mixtures with more than 24 and 19 percent hydrogen, respectively. The choking limit for these two conditions was found to be 14 and 16 percent hydrogen, respectively. The DDT and choking limits for hydrogen-air mixtures with 10 percent steam dilution at 400K were 18 and 12 percent hydrogen, respectively.

In general, the experiments performed for the tube diameter and orifice plate configuration studied indicate that:

- a. Increasing the initial temperature of hydrogen-air-steam mixtures at 0.1 MPa increased the likelihood of DDT (e.g., DDT was not observed in mixtures of hydrogen-air between 11 and 14 percent hydrogen at an initial temperature of 300K, whereas DDT was observed for these same mixtures at 650K). Thus, for severe accidents, the initial pre-combustion high temperature of a containment

6. Conclusions

compartment can have a significant impact on the hydrogen combustion mode and thus pressure loads.

- b. The DDT limit data could be correlated with the $d/\lambda=1$ criterion proposed by Peraldi et al. (1986). The exception was in the dry hydrogen-air mixtures at 650K, where the DDT limit was observed to be 11 percent hydrogen which corresponds to a value of $d/\lambda=5.5$. This DDT limit dropped to 9.5 percent hydrogen ($d/\lambda=4.2$) when the first 6.1 meters of the vessel was maintained at 400K with the rest of the vessel at 650K. This indicates that the experimentally measured DDT limit at 650K is not a fundamental detonation property and that the $d/\lambda=1$ DDT limit criterion provides a necessary but not sufficient condition for the onset of DDT in obstacle-laden ducts. In this particular case, the mixture initial condition (i.e., temperature) resulted in the inability of the mixture to sustain flame acceleration to the point where DDT could occur. This implies that when using the DDT criterion in a safety analysis (e.g., to obtain a lower detonability limit for a given compartment) the amount of conservatism built into this relation should be taken into account. Thus, if during a severe accident the dimensions and conditions of a containment compartment meet the criterion of $d/\lambda=1$, it does not necessarily mean that DDT will occur. It simply indicates that the necessary condition for DDT is met and transition could occur.

For severe accident analysis, when using the DDT limit criterion, one must consider that the containment compartment cross-section can accommodate not only one cell in the lateral dimension but also is long enough for significant flame acceleration leading to transition to detonation. Since the detonation run-up distance cannot simply be scaled, we can only qualitatively comment on the impact of temperature on the run-up distance. The tests have demonstrated that the cell size for a given hydrogen-air-steam mixture decreases with increasing initial temperature, and thus transition can occur in smaller compartments. However, the detonation run-up distance, which is governed primarily by flame acceleration, increases with increasing temperature. Theoretically, transition can occur in narrower containment compartments due to the cell size effect at higher initial temperatures. However, due to the influence of temperature on the run-up distance, the containment compartment may not be long enough for the required flame acceleration that leads to DDT.

7. REFERENCES

Beauvais, B., F. Mayinger, and G. Strube, "Severe Accident in a Light Water Reactor: Influence of Elevated Initial Temperature on Hydrogen Combustion," ASME/JSME Nuclear Engineering Conference-Volume 1, pp. 425-433, 1993.

Behrens, U., G. Langer, M. Stock, and I. Wirkner-Bott, "Deflagration-Detonation Transition in Hydrogen-Air-Steam Mixtures - Relevance of the Experimental Results for Real Accident Situations," Nuclear Engineering and Design, 130, pp. 43-50, 1991.

Berman, M., "Hydrogen Combustion Research at Sandia," Proceedings of the International Conference on Fuel-Air Explosions, Fuel-Air Explosions, University of Waterloo Press, Waterloo, Ontario, Canada, SM Study No. 16, p. 861, 1982.

Bollinger, L., L. Fong, R. Edse, "Experimental Measurement and Theoretical Analysis of Detonation Induction Distance," ARSJ, 31, p. 588, 1961.

Bollinger, L., "Experimental Detonation Velocities and Induction Distances in Hydrogen-Air Mixtures," AIAAJ, 2, p. 131, 1964.

Bradley, R.G., Lau, A.K.C., and Laws, M., Phil. Trans. R. Soc. London A338, p.359, 1992.

Chapman, W., and R. Wheeler, "The Propagation of Flame in Mixtures of Methane and Air, Part IV: The Effect of Restrictions in the Path of the Flame," J. Chem. Soc. (London), pp. 2139-2147, 1926.

Chu, R., J. Clark, and J. Lee, "Chapman-Jouget Deflagrations," Proceedings of the Royal Society London A, 441, pp. 607-623, 1993.

Ciccarelli, G., T. Ginsberg, J. Boccio, C. Economos, C. Finfrock, L. Gerlach, K. Sato, and M. Kinoshita, "High-Temperature Hydrogen-Air-Steam Detonation Experiments in the BNL Small-Scale Development Apparatus," NUREG/CR-6213, BNL-NUREG-52414, 1994.

Ciccarelli, G., T. Ginsberg, J. Boccio, C. Finfrock, L. Gerlach, and H. Tagawa, "Detonation Cell Size Measurements in High-Temperature Hydrogen-Air-Steam Mixtures at the BNL HTCF," NUREG/CR-6391, BNL-NUREG-52482, November 1997.

Desbordes, D., et al., "Failure of the Classical Dynamic Parameters Relationships in Highly Regular Cellular Detonation Systems," Progress of Astronautics and Aeronautics, 153, Dynamics of Explosions, pp. 347-359, 1993.

Dorofeev, S., et al., "Experimental Study on Hydrogen-Air Mixtures Combustion Behavior Under Turbulent Jet Ignition at Large Scale," RRCKI-80-05/3, VARGOS-93/1, 1992.

Dorofeev, S., et al., "DDT in Large Confined Volume of Lean Hydrogen-Air Mixtures," Combustion and Flame, Vol. 104 1/2, pp. 95, January 1996.

7. References

- Guirao, C., R. Knystautas, and J. Lee, "A Summary of Hydrogen-Air Detonation Experiments," NUREG/CR-4961, 1989.
- Holman, J., *Heat Transfer*, McGraw Hill, NY, 1981.
- Kumar, R., "Flammability Limits of Hydrogen-Oxygen-Diluent Mixtures," *J. Fire Sci.*, 3(4), pp. 245-262, 1985.
- Laffitte, P., "Influence of Temperature on the Formation of Explosive Waves," *Compt. Rendu*, 186, p. 951, 1928.
- Lee, J. H., "Dynamic Parameters of Gaseous Detonations," *Annual Review of Fluid Mechanics*, 16, pp. 311-336, 1984.
- Lee, J. H., R. Knystautas, and N. Yoshikawa, *Acta Astronautica*, 5, p. 971, 1978.
- Lefebvre A., and R. Reid, "The Influence of Turbulence on the Structure and Propagation of Enclosed Flames," *Combustion and Flame* 10, pp. 355-366, 1966.
- Liu, D., and R. MacFarlane, "Laminar Burning Velocities of Hydrogen-Air and Hydrogen-Air-Steam Flames," *Combustion and Flame*, 49: pp. 59-71, 1983.
- Meyer, J., and A. Oppenheim, "On the Shock-Induced Ignition of Explosive Gases," *Proceedings of the 13th International Symposium on Combustion*, pp. 1153-1163, 1971.
- Nettleton, M., "Gaseous Detonations," Chapman Hall, New York, 1987.
- Peraldi, O., Knystautas, R., and Lee, J.H., "Criteria for Transition to Detonation in tubes," *Proceedings of the 21st Symposium (International) on Combustion*, The Combustion Institute, Pittsburgh, 1986, pp. 1629-1637.
- Reynolds, W., "The Element Potential Method for Chemical Equilibrium Analysis: Implementation in the Interactive Program STANJAN Version 3," Dept. of Mechanical Engineering, Stanford University, Palo Alto, California, January 1986.
- Shchelkin, K., "Influence of Tube Roughness on the Formation and Detonation Propagation in Gases," *Zh. Exp. Teor. Fiz. (USSR)*, 10, pp. 823-827, 1940.
- Shepherd, J. E., "Chemical Kinetics of Hydrogen-Air-Diluent Detonations," *Progress of Astronautics and Aeronautics*, 106, Dynamics of Explosions, J.R. Bowen et al., eds., 1986.
- Shepherd, J. E., et al., "Analyses of the Cellular Structure of Detonations," *Twenty-first Symposium (International) on Combustion*, Combustion Institute, 1988.
- Sherman, M., M. Berman, and R. Beyer, "Experimental Investigation of Pressure and Blockage Effects on Combustion Limits in Hydrogen-Air-Steam Mixtures," SAND 91-0252, 1993.

7. References

Sherman, M., S. Tieszen, and W. Benedick, "Flame Facility, The Effect of Obstacles and Transverse Venting on Flame Acceleration and Transition to Detonation for Hydrogen-Air Mixtures at Large Scale," NUREG/CR-5275, 1989.

Teodorczyk, A., J. Lee, and R. Knystautas, "Photographic Studies of the Structure and Propagation Mechanism of Quasi-Detonations in Rough Tubes," Progress of Astronautics and Aeronautics, 134, Dynamics of Explosions, A. Kuhl et al., eds, 1991.

Thompson, P., *Compressible Fluid Dynamics*, McGraw-Hill, NY, 1972.

Urtiew, P., and A. Oppenheim, "Experimental Observations of the Transition to Detonation in an Explosive Mixture," Proc. of Royal Society London Series A, 295, pp. 13-28., 1966.

APPENDIX A

TABULATED DATA

The following table provides a summary of all the experiments performed in this test series. All test were performed at an initial pressure of 0.1 MPa. The data is grouped into seven test series consisting of tests performed at common initial temperatures, with and without steam dilution. In all cases, the quoted initial temperature has an uncertainty of $\pm 14\text{K}$ corresponding to the measured temperature uniformity from thermal calibration tests performed on the vessel. The hydrogen concentration, reported on a dry basis, is obtained from a single gas sample taken from the center of the vessel prior to ignition and analyzed using a gas chromatograph. Shown in the table is the average hydrogen concentration obtained from the gas sample. The steam dilution reported is a nominal value obtained from the set venturi constituent flow rates, no direct measurement of the steam dilution was made. Also given is the average combustion front velocity measured in roughly the second half of the vessel along with the standard deviation in the velocity data. The last column indicates the mode of propagation observed for each respective test. The following is a list of abbreviations and definitions used in the following tables.

- a = maximum velocity measured in the vessel.
- b = no gas sample obtained, value given based on nominal hydrogen and air venturi settings.
- c = velocity measured at end of the vessel.
- d = temperature rise only observed in first thermocouple, insufficient data acquisition time sweep.
- n/a = not available

Appendix A

Table A.1 Summary of initial thermodynamic conditions and measured combustion front velocity and pressure

TEST SERIES #1: Hydrogen-air mixtures at 300K

Test#	Hydrogen (%)	Velocity (m/s)		Pressure (atm)	Propagation mode
		average	sdv		
173	48.83	1954	16	14.7	detonation
10	29.94	1904	35	13.1	detonation
9	25.04	1730	31	16.3	detonation
8	19.97	1444	44	15.0	detonation
11	17.39	1248	44	10.9	detonation
12	15.91	1131	22	9.3	detonation
21	15.80	1116	10	12.0	detonation
13	14.97	1058	30	12.0	detonation
14	13.93	867	17	4.4	choking
19	13.83	843	50	3.3	choking
15	12.72	683	17	2.7	choking
16	11.83	644	8	2.3	choking
18	11.0 ^b	550	27	1.6	choking
132	10.02	254	a		deflagration
133	9.03	92	a		deflagration
135	8.57	127	a		deflagration
134	8.0 ^b	0			no ignition

TEST SERIES #2: Hydrogen-air mixtures at 500K

Test#	Hydrogen (%)	Velocity (m/s)		Pressure (atm)	Propagation mode
		average	sdv		
142	50.57	2062	47	8.0	detonation
54	30.59	1910	12	6.3	detonation
53	25.06	1777	12	6.3	detonation
43	20.13	1564	12	7.2	detonation
44	17.54	1447	22	5.7	detonation
45	15.18	1296	9	6.0	detonation
46	13.08	1159	25		detonation
57	12.10	1015	7	5.4	detonation
60	10.91	675		4.1	choking
129	9.82	696		2.0	choking
50	9.03	672		2.0	choking
51	8.80	686		2.4	choking
52	7.51	1.9 ^b			deflagration
53	7 ^b				no deflagration

Table A.1 Summary of initial thermodynamic conditions and measured combustion front velocity and pressure (cont'd)**TEST SERIES #3a: Hydrogen-air mixtures at 650K**

Test#	Hydrogen (%)	Velocity (m/s)		Pressure (atm)	Propagation mode
		average	sdv		
165	48.83	2041	32	6.8	detonation
33	30.29	1872	21	6.0	detonation
32	25.38	1764	27	5.9	detonation
31	20.02	1563 ^c		5.2	detonation
24	17.40	1450 ^c		4.8	detonation
38	15.04	1382	7	5.4	detonation
122	13.78	1264 ^c		4.1	detonation
121	12.80	1215 ^c		4.3	detonation
27	11.98	1181 ^c		4.8	detonation
35	12.02	1130 ^c		4.4	detonation
84	10.83	1227 ^c		4.9	detonation
29	11.15	1256 ^c		6.1	detonation
30	11.09	1333 ^c		1.8	detonation
34	10.5	120 ^a			deflagration
136	10	41 ^a			deflagration
123	9	15 ^a			deflagration
124	8	9 ^a			deflagration
138	7	1 ^a			deflagration
139	6	7 ^a			deflagration
141	5	0 ^a			no ignition

TEST SERIES #3b: Hydrogen-air mixtures at 650K with first 6.1 meters at 400K

Test#	Hydrogen (%)	Velocity (m/s)		Propagation mode
		average	sdv	
70	20.21	1624	16	detonation
68	13.96	1329	16	detonation
69	13.02	1277	25	detonation
71	11.94	1227	13	detonation
72	11.08	1188	33	detonation
73	10.10	1147	27	detonation
78	9.98	1119	20	detonation
75	9.51	1092 ^c		detonation
77	9.45	1100 ^c		detonation
76	8.93	d		deflagration

Appendix A

Table A.1 Summary of initial thermodynamic conditions and measured combustion front velocity and pressure (cont'd)

TEST SERIES #4: Hydrogen-air mixtures with 10 percent steam dilution at 400K

Test#	Hydrogen (%)	Velocity (m/s)		Pressure (atm)	Propagation mode
		average	sdv		
95	30.28	1712	9	8.3	detonation
96	25.24	1534	12	8.3	detonation
110	22.26	1385	21	8.2	detonation
97	20.20	1233	15	7.7	detonation
106	19.18	1143	11	10.6	detonation
98	18.19	1107	28	7.5	detonation
108	18.07	1036 ^c		5.9	detonation
100	17.21	779 ^c		2.1	deflagration
109	17.34	858 ^c		3.6	choking
99	16.05	739	28	2.7	choking
105	15.07	728	6	2.4	choking
101	14.12	721	26	2.9	choking
102	11.99	603 ^c		1.9	choking
170	10.95	381 ^a		0.9	deflagration
167	10.05	242 ^a			deflagration
169	9.59	271 ^a			deflagration
168	8.91	0			no ignition

TEST SERIES #5: Hydrogen-air mixtures with 25 percent steam dilution at 500K

Test#	Hydrogen (%)	Velocity (m/s)		Pressure (atm)	Propagation mode
		average	sdv		
143	30.37	1440	18	6.9	detonation
149	28.73	1332	15	8.6	detonation
148	26.28	1238	29	9.2	detonation
144	25.47	1192	15	8.0	detonation
151	24.37	1167	19	6.4	detonation
147	23.99	862	37	3.4	choking
152	23.25	842	27	2.0	choking
145	21.77	834	25	2.0	choking
153	20.08	790	15	2.0	choking
154	16.90	729 ^c		1.8	choking
155	14.84	677 ^c		1.7	choking
156	13.95	672 ^c		1.7	choking
158	13.25	237 ^a			deflagration
157	12.16	61 ^a			deflagration
159	11.19	1 ^a			deflagration
160	10 ^b	0			no ignition

Table A.1 Summary of initial thermodynamic conditions and measured combustion front velocity and pressure (cont'd)

TEST SERIES #6a: Hydrogen-air mixtures with 25 percent steam dilution at 650K

Test#	Hydrogen (%)	Velocity (m/s)		Pressure (atm)	Propagation mode
		average	sdv		
92	29.99	1512	23	5.7	detonation
85	25.57	1341 ^c		4.9	detonation
86	20.12	1106 ^c		5.7	detonation
127	18.71	1096 ^c		4.4	detonation
88	19.02	993 ^c		4.0	choking
93	18.96	954 ^c		3.9	choking
87	18.01	688 ^c		1.4	choking
94	18.04	692 ^c		1.6	choking
125	17.78	705 ^c		2.3	choking
126	16.77	800 ^c		2.1	choking
89	17.10	789 ^c		2.0	choking
91	15.96	872 ^c		2.3	choking
90	14.79	66 ^a			deflagration
161	12.27	3 ^a			deflagration
163	8.71	1 ^a			deflagration
164	4.52	0			no ignition

TEST SERIES #6b: Hydrogen-air mixtures with 25 percent steam dilution at 650K with first 6.1 meters at 400K

Test#	Hydrogen (%)	Velocity (m/s)		Pressure (atm)	Propagation mode
		average	sdv		
113	24.87	1390	19	n/a	detonation
115	21.46	1241	29	n/a	detonation
114	19.87	1133	19	n/a	detonation
117	19 ^b	995 ^c		n/a	detonation
118	17.85	740	31	n/a	choking
119	16.73	735	8	n/a	choking
120	16 ^b	735	17	n/a	choking

BIBLIOGRAPHIC DATA SHEET

(See instructions on the reverse)

2. TITLE AND SUBTITLE

The Effect of Initial Temperature on Flame Acceleration and Deflagration-to-Detonation Transition Phenomenon

1. REPORT NUMBER
(Assigned by NRC, Add Vol., Supp., Rev., and Addendum Numbers, if any.)

NUREG/CR-6509
BNL-NUREG-52515

5. AUTHOR(S)

G. Ciccarelli, J. L. Boccio, T. Ginsberg, C. Finfrock, L. Gerlach, Brookhaven National Laboratory
H. Tagawa, Nuclear Power Engineering Corporation
A. Malliakos, Nuclear Regulatory Commission

3. DATE REPORT PUBLISHED

MONTH	YEAR
May	1998

4. FIN OR GRANT NUMBER
L 1924/A3991

6. TYPE OF REPORT

Technical

7. PERIOD COVERED (Inclusive Dates)

8. PERFORMING ORGANIZATION - NAME AND ADDRESS (If NRC, provide Division, Office or Region, U.S. Nuclear Regulatory Commission, and mailing address; if contractor, provide name and mailing address.)

Brookhaven National Laboratory
Upton, NY 11973-5000

9. SPONSORING ORGANIZATION - NAME AND ADDRESS (If NRC, type "Same as above"; if contractor, provide NRC Division, Office or Region, U.S. Nuclear Regulatory Commission, and mailing address.)

Division of Systems Technology	Nuclear Power Engineering Corporation
Office of Nuclear Regulatory Research	5F Fujita Kanko Toranomon Building
U.S. Nuclear Regulatory Commission	3-17-1, Toranomon, Minato-Ku
Washington, DC 20555-0001	Tokyo 105, Japan

10. SUPPLEMENTARY NOTES

A. Malliakos, NRC Project Manager

11. ABSTRACT (200 words or less)

The High-Temperature Combustion Facility at BNL was used to conduct deflagration-to-detonation transition (DDT) experiments. Periodic orifice plates were installed inside the entire length of the detonation tube in order to promote flame acceleration. The orifice plates are 27.3-cm outer diameter, which is equivalent to the inner diameter of the tube, and 20.6-cm-inner diameter. The detonation tube length is 21.3-meters long, and the spacing of the orifice plates is one tube diameter. A standard automobile diesel engine glow plug was used to ignite the test mixture at one end of the tube. Hydrogen-air-steam mixtures were tested at a range of temperatures up to 650K and at an initial pressure of 0.1 MPa. It was also observed that the distance required for the flame to accelerate to the point of detonation initiation, referred to as the run-up distance, was found to be a function of both the hydrogen mole fraction and the mixture initial temperature. Decreasing the hydrogen mole fraction or increasing the initial mixture temperature resulted in longer run-up distances. The density ratio across the flame and the speed of sound in the unburned mixture were found to be two parameters which influence the run-up distance.

12. KEY WORDS/DESCRIPTORS (List words or phrases that will assist researchers in locating the report.)

detonation, deflagration-to-detonation transition, hydrogen air steam mixtures, flame acceleration, High Temperature Combustion Facility

13. AVAILABILITY STATEMENT

unlimited

14. SECURITY CLASSIFICATION

(This Page)

unclassified

(This Report)

unclassified

15. NUMBER OF PAGES

16. PRICE

M98005499



Report Number (14) NUREG /CR -- 6509

BNL - NUREG - 52515

Publ. Date (11) 199805

Sponsor Code (18) ~~NR~~ NRC , XF

UC Category (19) UC-000 , DOE/ER

mo 1332 in folder

19980706 070

DOE